nature medicine

ARTICLES

https://doi.org/10.1038/s41591-018-0275-4

Exercise-linked FNDC5/irisin rescues synaptic plasticity and memory defects in Alzheimer's models

Mychael V. Lourenco[1,2,3], Rudimar L. Frozza[1,4,19], Guilherme B. de Freitas[1,5,19], Hong Zhang[3], Grasielle C. Kincheski[1,2], Felipe C. Ribeiro[1,2], Rafaella A. Gonçalves[5], Julia R. Clarke[1,6], Danielle Beckman[1], Agnieszka Staniszewski[3], Hanna Berman[3], Lorena A. Guerra[1,2], Letícia Forny-Germano[1], Shelby Meier[7], Donna M. Wilcock[7], Jorge M. de Souza[8,9], Soniza Alves-Leon[8,9], Vania F. Prado[10,11,12], Marco A. M. Prado[10,11,12], Jose F. Abisambra[7], Fernanda Tovar-Moll[13,14], Paulo Mattos[13,15], Ottavio Arancio[3,16,17]*, Sergio T. Ferreira[1,2]* and Fernanda G. De Felice[1,5,18]*

Defective brain hormonal signaling has been associated with Alzheimer's disease (AD), a disorder characterized by synapse and memory failure. Irisin is an exercise-induced myokine released on cleavage of the membrane-bound precursor protein fibronectin type III domain-containing protein 5 (FNDC5), also expressed in the hippocampus. Here we show that FNDC5/irisin levels are reduced in AD hippocampi and cerebrospinal fluid, and in experimental AD models. Knockdown of brain FNDC5/irisin impairs long-term potentiation and novel object recognition memory in mice. Conversely, boosting brain levels of FNDC5/irisin rescues synaptic plasticity and memory in AD mouse models. Peripheral overexpression of FNDC5/irisin rescues memory impairment, whereas blockade of either peripheral or brain FNDC5/irisin attenuates the neuroprotective actions of physical exercise on synaptic plasticity and memory in AD mice. By showing that FNDC5/irisin is an important mediator of the beneficial effects of exercise in AD models, our findings place FNDC5/irisin as a novel agent capable of opposing synapse failure and memory impairment in AD.

The incidence of AD, the most common form of dementia in older individuals, is increasing as the world population ages, with more than 35 million people now affected worldwide[1]. Currently, there is no effective treatment for AD[2]; notable efforts are aimed at developing strategies to counteract mechanisms leading to neuronal damage, synapse failure, and memory impairment in AD.

Consolidated evidence indicates that the central nervous system (CNS) is an important target for the actions of peripheral hormones, including insulin, leptin, glucagon-like peptide-1, glucocorticoids, and others[3–5]. Insulin, leptin, and glucagon-like peptide-1 stimulate neuronal survival and synaptic plasticity, and they contribute to higher brain functions, including cognition[6–9]. Failure of hormone-initiated signaling pathways has been associated with brain disorders, including AD[10]. For example, brain insulin signaling is decreased in AD[4,11–13], and strategies aimed at bolstering it are currently under clinical investigation[14,15].

Irisin was recently identified as a myokine released into the circulation on physical exercise that is capable of stimulating adipocyte browning and thermogenesis in mice and humans[16,17]. Irisin is cleaved from fibronectin type III domain-containing protein 5 (FNDC5), a transmembrane precursor protein expressed in muscle under the control of peroxisome proliferator-activated receptor-γ coactivator 1α (PGC-1α). FNDC5/irisin stimulates the expression of brain-derived neurotrophic factor (BDNF) in the hippocampus[18], a brain region centrally involved in learning and memory. This raises the possibility that FNDC5/irisin could play a neuroprotective role in brain disorders such as AD. In this study, we investigated FNDC5/irisin levels in the brain and cerebrospinal fluid (CSF) of patients with AD and in mouse models of AD, and we tested the hypothesis that FNDC5/irisin could be a key mediator of the beneficial effects of exercise on synaptic plasticity and memory in AD models, thus holding promise as a potential target for therapeutic intervention in AD.

[1]Institute of Medical Biochemistry Leopoldo de Meis, Federal University of Rio de Janeiro, Rio de Janeiro, Brazil. [2]Institute of Biophysics Carlos Chagas Filho, Federal University of Rio de Janeiro, Rio de Janeiro, Brazil. [3]Taub Institute for Research on Alzheimer's Disease and the Aging Brain, Columbia University, New York, NY, USA. [4]Oswaldo Cruz Institute, Oswaldo Cruz Foundation, FIOCRUZ, Rio de Janeiro, Brazil. [5]Centre for Neuroscience Studies, Queen's University, Kingston, Ontario, Canada. [6]School of Pharmacy, Federal University of Rio de Janeiro, Rio de Janeiro, Brazil. [7]Sanders-Brown Center on Aging, University of Kentucky, Lexington, KY, USA. [8]Division of Neurosurgery, Clementino Fraga Filho University Hospital, Federal University of Rio de Janeiro, Rio de Janeiro, Brazil. [9]Division of Neurology/Epilepsy Program, Clementino Fraga Filho University Hospital, Federal University of Rio de Janeiro, Rio de Janeiro, Brazil. [10]Robarts Research Institute, University of Western Ontario, London, Ontario, Canada. [11]Department of Physiology and Pharmacology, University of Western Ontario, London, Ontario, Canada. [12]Department of Anatomy & Cell Biology, University of Western Ontario, London, Ontario, Canada. [13]D'Or Institute for Research and Education , Rio de Janeiro, Brazil. [14]Institute of Biomedical Sciences, Federal University of Rio de Janeiro, Rio de Janeiro, Brazil. [15]Institute of Psychiatry, Federal University of Rio de Janeiro, Rio de Janeiro, Brazil. [16]Department of Pathology & Cell Biology, Columbia University, New York, NY, USA. [17]Department of Medicine, Columbia University, New York, NY, USA. [18]Department of Psychiatry, Queen's University, Kingston, Ontario, Canada. [19]These authors contributed equally: Rudimar L. Frozza, Guilherme B. de Freitas. *e-mail: oa1@cumc.columbia.edu; ferreira@biof.ufrj.br; fernanda.defelice@queensu.ca

Results

Immunodetection of FNDC5/irisin in the brain. Since the original report[16] describing irisin as a cleavage product derived from FNDC5 (Fig. 1a), the existence and possible physiological functions of irisin in rodents and humans have been a matter of controversy. Part of the debate has focused on the specificity and identity of proteins identified using anti-FNDC5/irisin antibodies. The existence and levels of irisin in human plasma have been settled using state-of-the-art mass spectrometry analysis[17]. Here we initially validated the rabbit polyclonal antibody used in this study (anti-FNDC5; Abcam, catalog no. ab131390) against recombinant irisin produced in Chinese hamster ovary (CHO) cells (AdipoGen; catalog no. AG-40B-0136). In agreement with recent reports[19,20], previous incubation of the antibody with antigen at increasing molar ratios effectively blocked immunodetection of recombinant irisin in western blots (Extended Data Fig. 1a). We note, nonetheless, that because irisin is derived from FNDC5, immunological approaches to detect irisin inherently detect its precursor FNDC5 in samples in which the latter is also present. Moreover, irisin has been reported to exhibit an apparent molecular mass in the 22–32 kDa range resulting from dimerization and/or glycosylation[15,18–21]. This is similar to the molecular mass of FNDC5[16,21], making it difficult to discriminate between FNDC5 and irisin in immunoblots from tissue samples where both FNDC5 and irisin may be present. Thus, in the current study, we refer to FNDC5/irisin when describing results based on immunological detection of irisin in brain tissue homogenates. On the other hand, because irisin is thought to comprise the majority of secreted FNDC5/irisin[16], we refer to irisin when describing results obtained in CSF or plasma using an irisin enzyme-linked immunosorbent assay (ELISA) kit.

We used the anti-FNDC5 antibody to identify FNDC5/irisin in mouse hippocampal (Fig. 1b) and human cortical homogenates (Fig. 1c). Immunoblots showed a band at 29 kDa, within the range reported for irisin, which migrated with similar electrophoretic mobility as recombinant irisin (CHO cells; Adipogen; catalog no. AG-40B-0136) (Fig. 1b). Mass spectrometry analysis in this band identified a peptide with amino acid sequence DNEPNNNK, which is contained within FNDC5 (Extended Data Fig. 1b,c and Source Data 1). On the basis of mass spectrometry results and because this band (which we termed band 1) was detected at the same apparent molecular mass as recombinant irisin, we used band 1 for quantification of FNDC5/irisin levels in subsequent experiments. In addition, we detected immunopositive bands at apparent molecular masses of ~40, 58, and 75 kDa (bands 2, 3, and 4, respectively; Fig. 1b). To rule out the possibility that bands 2–4 could reflect nonspecific antibody labeling, we analyzed them by mass spectrometry. The results showed that bands 2 and 3 contained the same FNDC5 peptide as band 1. An additional peptide (DEVTMKEMGR) identified in band 4 was also comprised within FNDC5/irisin (Extended Data Fig. 1b,c and Source Data). The results indicate the presence of different forms of FNDC5/irisin (for example, multimers and/or posttranslationally modified species) in immunoblots from brain homogenates.

FNDC5/irisin is reduced in AD brains and CSF, and in AD experimental models. FNDC5/irisin was significantly reduced in the hippocampi of late-stage AD patients compared to age-matched early AD or cognitively normal individuals (Fig. 1d,e; see Supplementary Table 1 for demographics). No changes were detected in βIII-tubulin (Tuj1), used as a neuron-specific control, indicating that the decrease in FNDC5/irisin was not caused by significant neuronal death in the samples analyzed (data not shown).

For CSF analysis of AD or control individuals, we employed an irisin ELISA kit (Phoenix Pharmaceuticals; catalog no. EK-067-29), which robustly recognizes recombinant irisin (Extended Data Fig. 1d). Irisin was decreased in the CSF of AD patients compared to mild cognitive impairment (MCI) or nondemented controls (Fig. 1f). Lewy body dementia (LBD) patients also presented reduced levels of irisin in the CSF (Fig. 1f). No significant alterations were found in plasma levels of irisin in AD or LBD patients compared to non-demented controls (Fig. 1g). CSF irisin levels showed a positive correlation with age in non-demented controls, but not in AD patients (Fig. 1h,i). While we found no correlation between CSF and plasma irisin levels in controls or AD patients (Extended Data Fig. 2a,b), we found a selective reduction in the CSF/plasma ratio of irisin in AD patients, but not in MCI or LBD patients (Extended Data Fig. 2c).

Next, we sought to determine whether amyloid-β oligomers (AβOs), soluble Aβ aggregates that accumulate in AD brains and are linked to synapse failure and memory loss[2,22], impact FNDC5/irisin levels. Exposure of rat hippocampal cultures to AβOs (500 nM; 24 h), reduced FNDC5/irisin at both messenger RNA (mRNA) (Extended Data Fig. 3a) and protein (Extended Data Fig. 3b,c) levels. FNDC5/irisin immunoreactivity was mostly associated with the surface of mature neurons (positively labeled for βIII-tubulin), with little immunoreactivity present in glial fibrillary acidic protein (GFAP)-positive astrocytes (Extended Data Fig. 3d,e). FNDC5/irisin immunoreactivity was reduced in AβO-exposed hippocampal cultures (Extended Data Fig. 3f,g). Specificity of surface staining by the anti-FNDC5 antibody was confirmed by our observation that lentivirus-mediated short hairpin RNA (shRNA) knockdown of FNDC5 markedly reduced its surface immunostaining (Extended Data Fig. 3h). We next exposed cultured human adult cortical slices[23] to AβOs (500 nM) for 12 h and observed that mRNA and protein levels of FNDC5/irisin were reduced (Fig. 2a–c).

Consistent with previous reports[18,24], we found that FNDC5/irisin is expressed in the hippocampus and cortex of C57BL/6 mice, albeit at lower levels than in skeletal muscle (Extended Data Fig. 4a). Intracerebroventricular infusion of AβOs (10 pmol in a single dose)[25,26] in C57BL/6 mice caused a significant reduction in hippocampal (Extended Data Fig. 4b,c), but not in skeletal muscle FNDC5/irisin mRNA (Extended Data Fig. 4d,e) after 24 h or 7 days. FNDC5/irisin protein levels detected by ELISA were reduced in the hippocampi of mice 24 h post-infusion of AβOs (Fig. 2d). FNDC5/irisin levels were also reduced in the hippocampi of 13- to 16-month-old APPswe/PS1ΔE9 mice (henceforth referred to as APP/PS1 ΔE9) (Fig. 2e,f), which develop amyloid pathology and memory deficits[27]. Taken together, our results indicate that FNDC5/irisin is expressed in the hippocampus and is reduced in AD brains and CSF, as well as in experimental models of AD.

Because FNDC5/irisin levels are controlled by PGC-1α[16], known to mediate synapse function and neuroprotection[28], we investigated PGC-1α and peroxisome proliferator-activated receptor gamma (PPAR-γ) expression in AβO-infused mice. Expression of both PGC-1α (Extended Data Fig. 4f,g) and PPAR-γ (Extended Data Fig. 4h,i), but not of peroxisome proliferator-activated receptor alpha (Extended Data Fig. 4j,k), were reduced in mouse hippocampi 24 h and 7 days post-infusion with AβOs. PGC-1α protein levels were also reduced 7 days post-infusion (Extended Data Fig. 4l,m).

Knockdown of brain FNDC5/irisin impairs synaptic plasticity and memory in mice. We infused C57BL/6 mice intracerebroventricularly with lentiviruses harboring two different shRNA constructs that efficiently knocked down FNDC5 (Fig. 3a,b). This resulted in impaired maintenance of hippocampal long-term potentiation (LTP) (Fig. 3c,d) and memory in a novel object recognition (NOR) task (Fig. 3e). Mice infected with a control lentiviral vector (harboring an shRNA targeting luciferase) exhibited normal performance in the NOR task (Fig. 3e). Downregulation of brain FNDC5/irisin had no impact on performance in the radial arm water maze (RAWM) or contextual fear conditioning (CFC) tasks in wild-type mice (Fig. 3f,g). Control experiments showed that

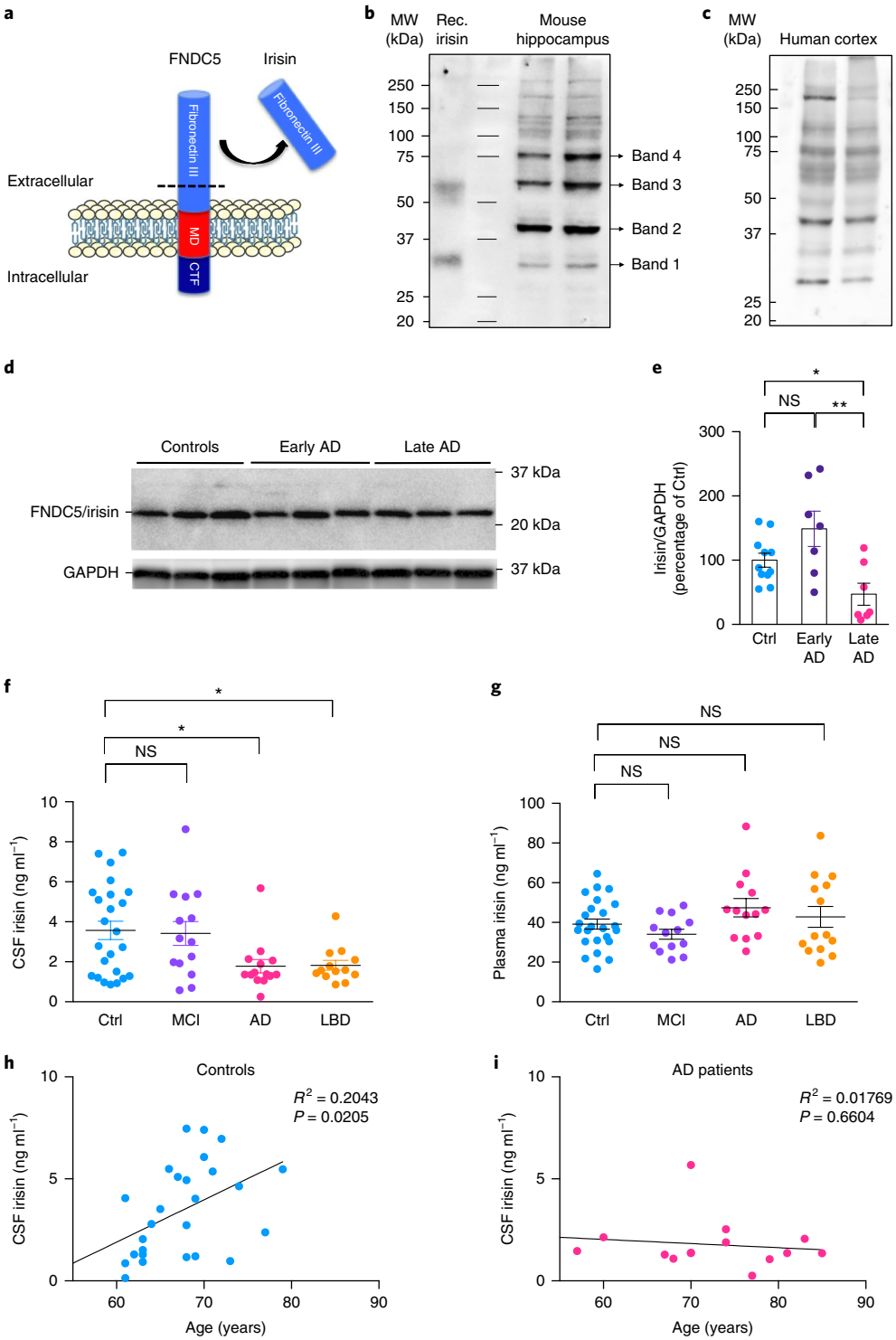

Fig. 1 | CNS FNDC5/irisin is reduced in AD. a, Schematic representation of FNDC5 containing irisin, as part of the fibronectin III domain, which is cleaved by proteolysis and released to the extracellular medium. MD, membrane domain. CTF, C-terminal fragment. **b**,**c**, Representative immunoblots of FNDC5 in the mouse hippocampus (**b**) and human cortex (**c**). Bands analyzed by mass spectrometry (see Extended Data Fig. 1 and Source Data 1) are indicated. These western blots were repeated three times with similar results. **d**,**e**, Summary quantification of human hippocampal irisin protein levels in late-stage AD or early AD cases compared with healthy controls ($N = 11$ controls, 7 early AD, 7 late AD); $^{*}P < 0.05$; $^{**}P < 0.01$, two-sided one-way ANOVA with Holm–Šidák post-test. Values are expressed as mean ± s.e.m. The experiments were repeated twice with similar results. See Source Data 2 for original data. **f**, Summary quantification of irisin in the CSF of AD and LBD patients compared with healthy controls or MCI patients ($N = 26$ controls, 14 MCI, 14 AD, 13 LBD patients); $^{*}P < 0.05$, two-sided one-way ANOVA followed by Holm–Šidák post-test. Center values are expressed as mean ± s.e.m. **g**, Plasma levels of irisin in AD and LBD patients compared to healthy controls or MCI patients ($N = 26$ controls, 13 MCI, 13 AD, 14 LBD patients). **h**,**i**, Correlation between age and CSF irisin in control ($N = 31$) and AD patients ($N = 14$); linear regression, R^2 and P values as indicated).

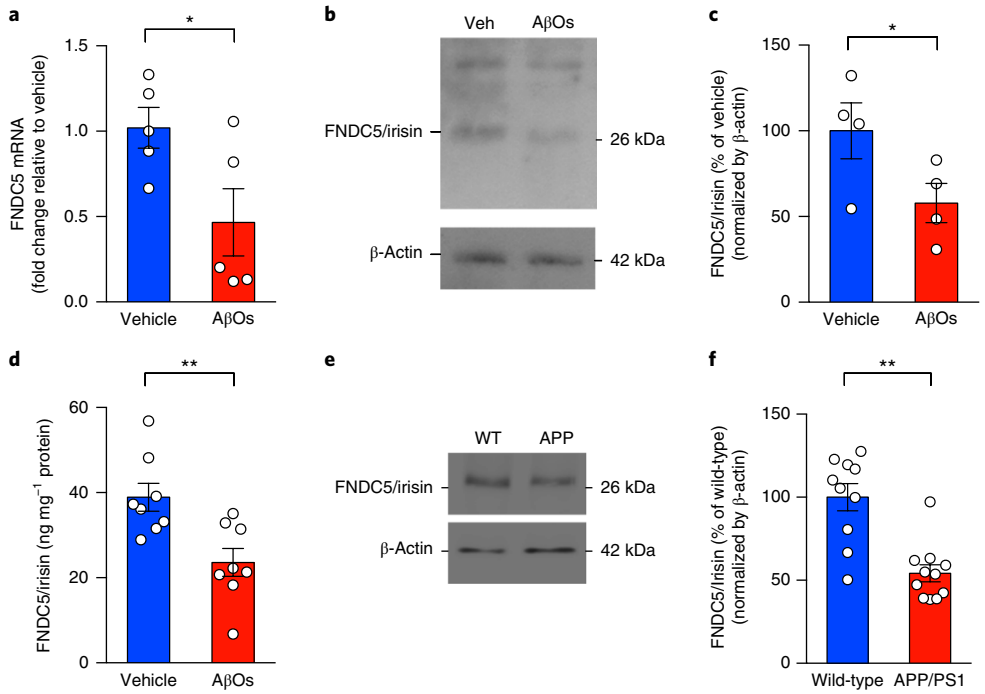

Fig. 2 | Brain FNDC5/irisin is reduced in AD models. a, FNDC5 mRNA levels in control (vehicle) and AβO-exposed human adult cortical slices after 12 h of treatment ($N = 5$ independent tissue donors for mRNA; $N = 4$ donors for protein levels; $^*P < 0.05$, two-sided paired Student's *t*-test; two-sided). **b**,**c**, Irisin levels in control (vehicle) and AβO-exposed human adult cortical slices after 12 h of treatment ($N = 5$ independent tissue donors for mRNA; $N = 4$ donors for protein levels; $^*P < 0.05$, two-sided paired Student's *t*-test). Irisin levels were normalized by β-actin. The experiments were repeated three times with similar results. See Source Data 3 for original data. **d**, ELISA quantification of hippocampal irisin levels in wild-type C57BL/6 mice 24 h post-AβO infusion ($N = 8$ mice per group, $^{**}P < 0.01$, two-sided paired Student's *t*-test). The experiments were repeated twice with similar results. **e**,**f**, Hippocampal levels of irisin in 13- to 16-month-old APP/PS1 ΔE9 mice ($N = 10$ for wild-type and 11 for APP/PS1 ΔE9 mice, $^{**}P < 0.01$, two-sided paired Student's *t*-test). The experiments were repeated twice with similar results. See Source Data 4 for original data. Bars express mean ± s.e.m. Source data 3 and 4.

lentivirus-infected mice showed no significant differences in motor activity or body weight (Extended Data Fig. 5a–c). Thus, results indicate that while brain FNDC5/irisin does not contribute to CFC and RAWM memory, it influences hippocampal synaptic plasticity and NOR memory in C57BL/6 mice.

Boosting brain FNDC5/irisin levels rescues synapse plasticity and memory defects in mouse models of AD. We next observed that recombinant irisin rescued impaired LTP in AβO-exposed hippocampal slices (Fig. 4a,b). Further, bilateral intrahippocampal infusion of recombinant irisin (75 pmol per site) prevented AβO-induced impairment in NOR and fear conditioning memory (Extended Data Fig. 6a,b).

To further explore whether FNDC5/irisin could counteract the direct impact of AβOs on memory[25,26], C57BL/6 mice were infected intracerebroventricularly with a green fluorescent protein (GFP) control vector (AdGFP) or with AdFNDC5, an adenoviral vector that overexpresses FDNC5. Six days post-infection, mice received a single intracerebroventricular infusion of AβOs (or vehicle). Control measurements showed that neither viral infection nor AβO infusion caused any changes in speed or distance traveled, or in the time spent at the center or periphery in an open field test (data not shown), indicating lack of effects on locomotor activity and anxiety. Brain expression of FNDC5/irisin blocked the AβO-induced alterations on both NOR (Fig. 4c) and CFC memory tests (Fig. 4d). Infection with AdFNDC5 led to increases in FNDC5/irisin mRNA expression and protein levels in the cortex (Fig. 4e,f) and hippocampus 6 days post-infection (Fig. 4g,h).

We further used a quantitative PCR (qPCR) array to interrogate hippocampal gene expression related to synaptic plasticity in mice previously infected with either AdGFP or AdFNDC5 and subsequently infused with vehicle or AβOs. Among 84 genes analyzed, AdFNDC5 rescued AβO-induced changes in expression of six genes, whose expression levels were independently validated by qPCR. These genes included immediate early genes (*Egr1*, *Egr4*) and genes coding for the protein phosphatase calcineurin (*Ppp3ca*), neuronal pentraxin 2 (*Nptx2*), and subunits of α-amino-3-hydroxy-5-methyl-4-isoxazolepropionic acid and metabotropic glutamate receptors (*Gria2*, *Grm2*) (Extended Data Fig. 7), indicating possible protective actions of FNDC5/irisin against aberrant expression of synapse-related genes.

Next, we intracerebroventricularly infused APP/PS1 ΔE9 mice[27] or wild-type mice with the AdFNDC5 vector or with AdGFP as a control and evaluated synaptic plasticity and memory. Fourteen days post-infection, after completion of behavioral experiments, acute hippocampal slices were prepared, and CA3–CA1 synapses were stimulated for LTP induction. While hippocampal slices from APP/PS1 ΔE9 mice infected with AdGFP exhibited impaired LTP (Fig. 4i,j), slices from APP/PS1 ΔE9 mice intracerebroventricularly infused with AdFNDC5 presented normal LTP (Fig. 4i,j). Brain expression of FNDC5/irisin rescued memory impairment in APP/PS1 ΔE9 mice in both RAWM (Fig. 4k) and CFC (Fig. 4l). Similar results in LTP, RAWM, and CFC were obtained with APP/PS1 M146L mice, another mouse model of AD[29] (Extended Data Fig. 8a–d). Control experiments showed that brain expression of FNDC5/irisin had no impact on locomotor activity, somatosensory behavior or body weight in APP/PS1 M146L mice (data not shown). Overall, results indicate that expression of FNDC5/irisin rescued hippocampal synaptic plasticity and memory in AD mice.

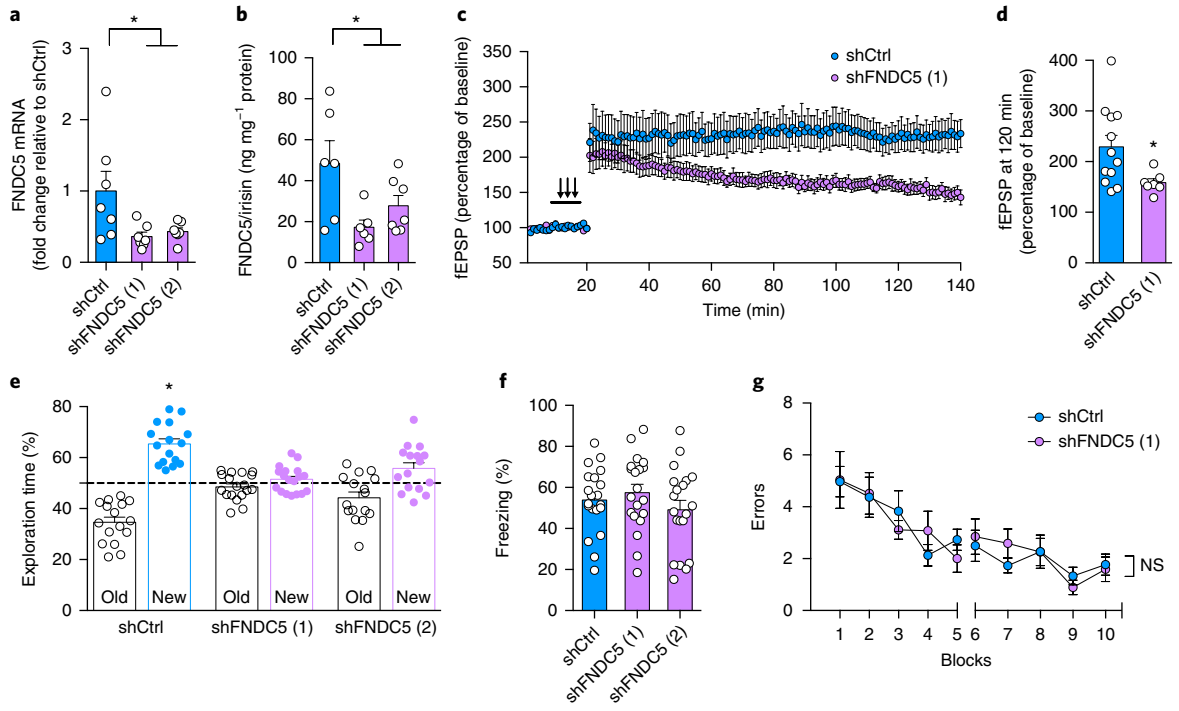

Fig. 3 | Downregulation of brain FNDC5/irisin impairs synaptic plasticity and object recognition memory in mice. Two distinct shRNAs targeting FNDC5 (shFNDC5 1 or 2) or shCtrl were injected intracerebroventricularly in C57BL/6 mice. **a**, Levels of FNDC5 mRNA compared to shFNDC5 (1)- or shFNDC5 (2)-injected mice ($N=7$ mice per group; $^*P<0.05$, one-way ANOVA with Holm–Šidák correction) in the frontal cortex. Bars express mean ± s.e.m. **b**, FNDC5/irisin protein in control (shCtrl) compared to shFNDC5 (1)- or shFNDC5 (2)-injected mice ($N=7$ mice per group; $^*P<0.05$, one-way ANOVA with Holm–Šidák correction) in the frontal cortex. Bars express mean ± s.e.m. **c**, Average traces for field excitatory postsynaptic potentials (fEPSPs) in hippocampal slices from each experimental group ($N=12$ slices for shCtrl, 7 slices for shFNDC5 (1) obtained from 3–4 mice per group). Traces represent mean ± s.e.m. per time. **d**, fEPSP at 120 min ($N=12$ slices for shCtrl, 7 slices for shFNDC5 obtained from 3–4 mice per group; $^*P<0.05$, two-sided repeated measures two-way ANOVA with Holm–Šidák correction). **e**, Summary quantification of novel object discrimination in the NOR task in shCtrl, shFNDC5 (1)- or shFNDC5 (2)-injected mice. $^*P<0.05$, statistically different from 50% (chance level) ($N=16$ mice for shCtrl, 18 for shFNDC5 (1), 16 for the shFNDC5 (2) group; one-sample Student's *t*-test). **f**, CFC in shCtrl or shFNDC5-infused C57BL/6 mice ($N=20$ mice per group; no significant difference was observed). Two-sided one-way ANOVA followed by Holm–Šidák correction. Bars express mean ± s.e.m. **g**, shCtrl or shFNDC5 (1)-infused C57BL/6 mice were assessed in a two-day RAWM task and presented similar error profiles across trials. Each block consisted of three consecutive trials. $N=9$ shCtrl, 11 shFNDC5 (1); repeated measures two-way ANOVA. Values are presented as mean ± s.e.m.

Neuroprotective actions of recombinant irisin in vitro. Because abnormal eukaryotic initiation factor 2α (eIF2α) phosphorylation and inhibition of protein synthesis have been recently described as key mechanisms driving synapse damage and memory failure in AD models[10,26,30–32], we examined the effects of recombinant irisin on phosphorylated eIF2α (eIF2α-P) and activating transcription factor 4 (ATF4) levels in cultured primary hippocampal neurons. Irisin prevented AβO-induced elevation in eIF2α-P and ATF4 (Extended Data Fig. 9a–c), as well as downregulation of de novo protein synthesis in hippocampal neurons (Extended Data Fig. 9d,e). Control measurements revealed that total eIF2α immunoreactivity remained unchanged (not shown).

We further found that recombinant irisin prevented dendritic spine loss in cultured hippocampal neurons exposed to AβOs (Extended Data Fig. 9f,g). Additional experiments determined that recombinant irisin reduced AβO binding to neurons (Extended Data Fig. 9h,i). Control binding studies revealed no direct interaction between AβOs and recombinant irisin (Extended Data Fig. 9j), ruling out the possibility that blockade of binding to neurons might be caused by sequestration of AβOs by recombinant irisin added to the medium. In addition, surface FNDC5/irisin and AβOs did not colocalize in dendrites of hippocampal neurons (Extended Data Fig. 9k). Results further showed that FNDC5/irisin overexpression reduced hippocampal soluble Aβ42 levels in APP/PS1 M146L mice (Extended Data Fig. 9l), but not insoluble Aβ42 in the hippocampus or cortex (Extended Data Fig. 9m–o).

We found that recombinant irisin stimulated the cyclic AMP (cAMP)–protein kinase A (PKA)–cAMP responsive element-binding protein (CREB) pathway in human cortical slices (Fig. 5a–c), a pathway that plays important roles in memory formation and has been found to be impaired in AD models[33–35]. Recombinant irisin further increased cAMP and phosphorylated CREB in mouse hippocampal slices (Fig. 5d,e). Irisin-induced CREB phosphorylation was abolished by PKA inhibition with myristoylated protein kinase inhibitor (PKI) 14–22, a selective PKA inhibitor (Fig. 5e). We also found that PKA activity mediated protection against nuclear translocation of ATF4 induced by AβOs (Fig. 5f,g). Irisin further induced transient phosphorylation of extracellular signal-regulated kinase in cultured neurons (data not shown). The effect of recombinant irisin was similar to forskolin, a direct activator of adenylyl cyclase (data not shown). Taken together, these results provide initial clues into the mechanisms by which recombinant irisin affords neuroprotection in experimental models of AD.

FNDC5/irisin mediates the protective actions of physical exercise on synaptic plasticity and memory in AD models. From a translational perspective, physical exercise could be a non-pharmacological strategy to increase hippocampal FNDC5/irisin in patients at

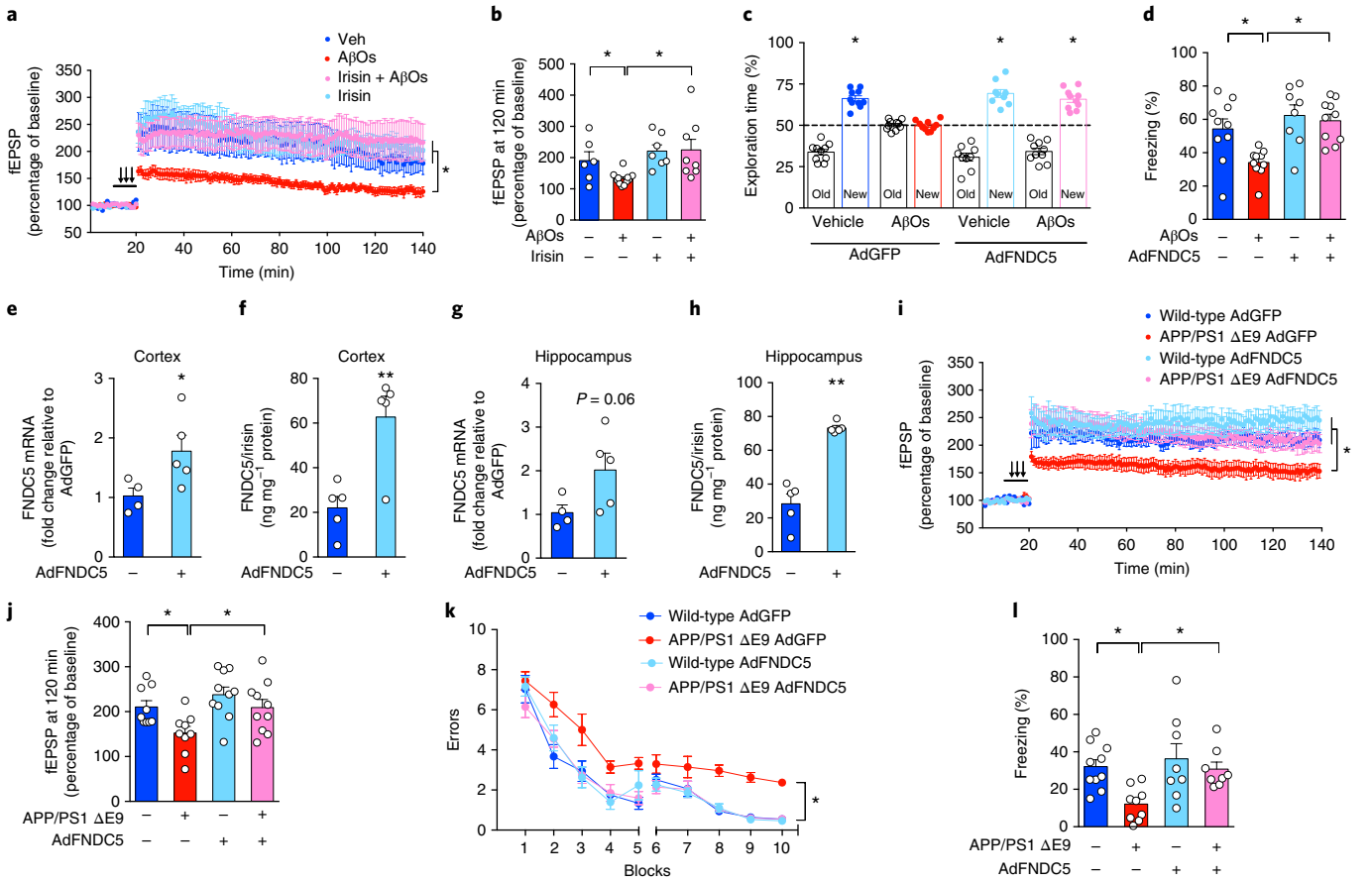

Fig. 4 | Brain FNDC5/irisin rescues defective synaptic plasticity and memory in AD mice. a,**b**, LTP measurement in hippocampal slices ($N=6$ slices for vehicle, 11 for AβOs, 7 for irisin, 8 for irisin + AβOs; slices were from 4 animals for each condition). **b**, fEPSP at 120 min ($N=6$ slices for vehicle, 11 for AβOs, 7 for irisin, 8 for irisin + AβOs; $^*P<0.05$, two-sided two-way ANOVA with Holm–Šidák correction). Values are presented as mean ± s.e.m. **c**,**d**, Effect of intracerebroventricular injection of AdFNDC5 on memory impairment in AβO-infused C57BL/6 mice in the NOR (**c**) and CFC (**d**) tasks ($N=10$ mice for vehicle GFP, 10 for AβOs GFP, 8 for vehicle FNDC5, 10 for AβOs FNDC5; $^*P<0.05$, statistically different from 50% (chance level) one-sample Student's *t*-test). Bars are presented as mean ± s.e.m. **e**,**f**, Cortical FNDC5 mRNA and protein expression in C57BL/6 mice 6 days after intracerebroventricular injection of AdGFP or AdFNDC5 vectors ($N=4$ mice for AdGFP, 5 for AdFNDC5; Student's *t*-test; $^*P<0.05$). **g**,**h**, Hippocampal FNDC5 mRNA and protein expression in C57BL/6 mice 6 days after intracerebroventricular injection of AdGFP or AdFNDC5 vectors ($N=4$ mice for AdGFP, 5 for AdFNDC5; $^*P<0.05$; two-sided Student's *t*-test. Bars are presented as mean ± s.e.m. **i**–**j**, APP/PS1 ΔE9 mice (or wild-type littermates) were injected intracerebroventricularly with an adenoviral vector expressing full-length FNDC5 (AdFNDC5) or AdGFP, used as a control. **i**, Average traces for fEPSPs in hippocampal slices from each experimental group ($N=10$ slices for wild-type AdGFP, 9 APP/PS1 ΔE9 AdGFP, 10 wild-type AdGFP, 10 APP/PS1 ΔE9 AdFNDC5; from 4 animals per group). Traces represent mean ± s.e.m. **j**, fEPSP at 120 min ($N=10$ slices for wild-type AdGFP, 9 APP/PS1 ΔE9 AdGFP, 10 wild-type AdGFP, 10 APP/PS1 ΔE9 AdFNDC5; from 4 animals per group; $^*P<0.05$, two-sided one-way ANOVA with Holm–Šidák correction). **k**,**l**, Effects of intracerebroventricular injection of AdFNDC5 on memory impairment in 3–4-month-old APP/PS1 ΔE9 mice in a two-day RAWM (**k**) and in CFC (**l**) ($N=10$ mice for wild-type AdGFP, 8 for APP/PS1 ΔE9 AdGFP, 11 for wild-type AdFNDC5, 10 for APP/PS1 ΔE9 AdFNDC5). $^*P<0.05$, two-sided two-way ANOVA with Holm–Šidák correction). Data are represented by mean ± s.e.m.

risk of developing AD or in patients already exhibiting cognitive impairment. Thus, we initially tested whether a protocol of daily swimming (1 h per day, 5 days per week for 5 weeks) could protect mice from AβO-induced memory deficits and reduction in brain levels of FNDC5/irisin. Notably, exercised mice were protected from AβO-induced impairment in NOR memory both 24 h (Extended Data Fig. 10a) and 5 days (Extended Data Fig. 10b) following AβO infusion. Protection against AβO-induced memory deficits was also verified in the CFC paradigm (Extended Data Fig. 10c).

We further found that this exercise protocol prevented AβO-induced reductions in FNDC5/irisin mRNA (Extended Data Fig. 10d) and protein (Extended Data Fig. 10e) in mouse hippocampi. Moreover, consistent with a previous report[18], hippocampal levels of FNDC5/irisin (Extended Data Fig. 10e) and BDNF (Extended Data Fig. 10f,g) were higher in exercised mice compared to sedentary animals.

We then asked whether brain FNDC5/irisin mediated the beneficial effect of physical exercise on synapse plasticity in APP/PS1 ΔE9 mice. We conducted an intracerebroventricular infusion of a lentiviral vector harboring FNDC5 shRNA and subsequently subjected mice to the exercise protocol. Results revealed that exercise improved LTP in APP/PS1 ΔE9 mice infused with an innocuous shRNA (targeting luciferase), but not in APP/PS1 ΔE9 mice exhibiting downregulated brain FNDC5/irisin expression (Fig. 6a,b). Additionally, we observed that downregulation of brain FNDC5/irisin did not exacerbate LTP impairment in sedentary APP/PS1 ΔE9 mice (Fig. 6a,b).

We next aimed to determine a potential role of peripheral FNDC5/irisin in the brain. We administered the AdFNDC5 vector into the caudal vein of mice to induce peripheral FNDC5/irisin expression, as previously described[18]. Peripheral administration of AdFNDC5 rescued NOR memory defects in AβO-infused mice

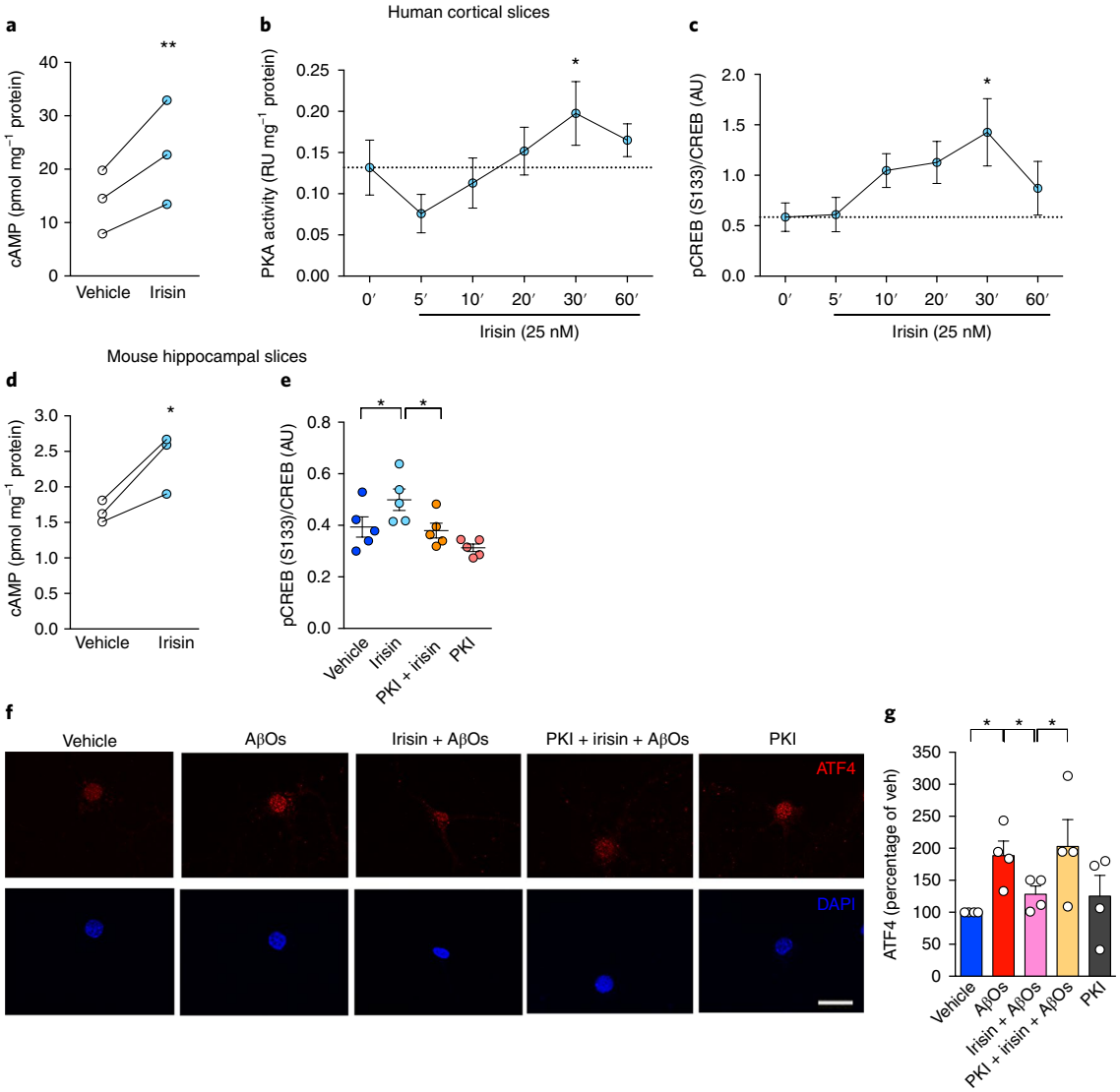

Fig. 5 | Irisin triggers the brain cAMP–PKA–CREB signaling pathway. a–d, Summary quantification of the effect of irisin (25 nM) on cAMP accumulation (**a**), PKA activation (**b**), and CREB phosphorylation (**c**) in human cortical slices ($N = 3$ independent experiments with slices from different tissue donors for cAMP and pCREB, and 4 for the PKA assay; $^{*}P < 0.05$; $^{**}P < 0.01$; two-sided repeated measures ANOVA). Data are represented by mean ± s.e.m. **d**, Analysis of cAMP accumulation induced by irisin (25 nM) in mouse hippocampal slices ($N = 4$ independent experiments with 6–8 slices from 4 independent animals; $^{*}P < 0.05$; two-sided paired Student's *t*-test). **e**, Analysis of pCREB activation induced by irisin ($N = 2$ independent experiments with 5 slices from 3 animals; $^{*}P < 0.05$; two-sided two-way ANOVA with Holm–Šidák correction). Data are represented by mean ± s.e.m., *N* defined per slice. **f**, Nuclear ATF4 levels (red) in primary cultures exposed to AβOs and/or irisin in the presence of PKI 14–22, a PKA selective inhibitor. Nuclei were counterstained in blue (DAPI). Scale bar, 10 µm. **g**, Summary quantification of immunocytochemistry experiments ($N = 4$ experiments with independent neuronal cultures and AβO preparations; 30 images (from 2–3 coverslips) per experimental condition per experiment). $^{*}P < 0.05$; two-sided paired two-way ANOVA with Holm–Šidák correction. Data are represented by mean ± s.e.m.

(Fig. 6c). We next evaluated plasma levels of FNDC5/irisin in this group of mice and found unaltered levels in AβO-infused animals (Fig. 6d). As expected, plasma levels of FNDC5/irisin were increased in animals that received AdFNDC5 intravenously (Fig. 6d). Moreover, while hippocampal levels of FNDC5/irisin were decreased in AβO-infused mice, intravenous injection of AdFNDC5 resulted in increased hippocampal FNDC5/irisin levels and prevented the decrease triggered by AβOs (Fig. 6e). These results suggest that peripheral FNDC5/irisin can either reach the brain or trigger an increase in brain FNDC5/irisin. They further demonstrate that peripheral FNDC5/irisin affords protection against AβO-induced memory impairment.

Our second approach to investigate the role of peripheral FNDC5/irisin in synaptic plasticity and memory in AD models consisted of neutralizing peripheral FNDC5/irisin. To this end, we carried out intraperitoneal injections of anti-FNDC5 antibodies in either sedentary or exercised AβO-infused mice. This approach has been previously described to attenuate irisin-induced expression of pro-thermogenesis genes in mice[16]. Interestingly, intraperitoneal administration of anti-FNDC5 blocked the protective actions of physical exercise against the impairments in synaptic plasticity and memory induced by AβOs (Fig. 6f,g). We further noted that intraperitoneal administration of the anti-FNDC5 antibody per se impaired synaptic plasticity and performance in the NOR test (Fig. 6f,g). We next aimed to evaluate the effects of exercise and peripheral administration of anti-FNDC5 on hippocampal FNDC5/irisin levels. In accordance with the results in Extended Data Fig. 10, we found that exercise prevented the decrease in hippocampal

Fig. 6 | FNDC5/irisin mediates the beneficial effects of exercise on synaptic plasticity and memory. a,**b**, APP/PS1 ΔE9 mice (or wild-type littermates) were injected intracerebroventricularly with a lentiviral vector expressing an shRNA targeting FNDC5 (shFNDC5) or an shRNA targeting luciferase (shCtrl, used as a control) and were exercised. **a**, Average traces for fEPSPs in hippocampal slices from each experimental group ($N=12$ slices for wild-type shCtrl sedentary, 11 for APP/PS1 ΔE9 shCtrl sedentary, 9 for APP/PS1 ΔE9 shCtrl exercised, 14 for APP/PS1 ΔE9 shFNDC5 exercised, 12 for APP/PS1 ΔE9 shFNDC5 sedentary; from 4 animals per group). Traces are represented by mean ± s.e.m. **b**, fEPSP at 120 min. $^*P<0.05$, two-way ANOVA with Holm–Šidák correction. ($N=12$ slices for wild-type shCtrl sedentary, 11 for APP/PS1 ΔE9 shCtrl sedentary, 9 for APP/PS1 ΔE9 shCtrl exercised, 14 for APP/PS1 ΔE9 shFNDC5 exercised, 12 for APP/PS1 ΔE9 shFNDC5 sedentary; from 4 animals per group; $^*P<0.05$, two-sided one-way ANOVA with Holm–Šidák correction). Values are represented by mean ± s.e.m. **c**, Effect of intravenously administered AdFNDC5 on NOR memory in AβO-infused mice 24 h after oligomer infusion ($N=11$ vehicle AdGFP; 9 AβOs AdGFP; 12 vehicle AdFNDC5; 9 AβOs AdFNDC5; $^*P<0.05$, statistically different from 50% (chance level) one-sample Student's *t*-test). Values are represented by mean ± s.e.m. **d**,**e**, Effect of intravenous AdFNDC5 administration on plasma ($N=5$ mice for vehicle AdGFP, 5 AβOs AdGFP, 5 vehicle AdFNDC5, 4 AβOs AdFNDC5) (**d**) and hippocampal (**e**) FNDC5/irisin levels (10 vehicle AdGFP, 11 AβOs AdGFP, 10 vehicle AdFNDC5, 7 AβOs AdFNDC5; $^*P<0.05$, two-sided two-way ANOVA with Holm–Šidák correction). Values are represented by mean ± s.e.m. **f**,**g**, AβO-injected mice were injected intraperitoneally with an anti-FNDC5 antibody and exercised. They were tested on synaptic plasticity and NOR memory 72 h after AβO infusion. **f**, Summary quantification of fEPSP at 120 min ($N=10$ slices for vehicle, 9 for AβOs, 11 for exercised, 11 for exercise + AβOs, 10 for anti-FNDC5, 10 for anti-FNDC5 + exercised + AβOs; from 4 animals per group; $^*P<0.05$, two-sided one-way ANOVA with Holm–Šidák correction). Values are represented by mean ± s.e.m. **g**, NOR performed 72 h after AβO infusion ($N=10$ mice for vehicle, 11 for AβOs, 12 for intraperitoneal anti-FNDC5, 8 for exercised, 12 for exercised + AβOs, and 12 for intraperitoneal anti-FNDC5 + exercised + AβOs); $^*P<0.05$; one-sample *t*-test. Values are represented by mean ± s.e.m. **h**, Analysis of intraperitoneal injections of anti-FNDC5 on exercise-induced hippocampal FNDC5/irisin levels in AβO-infused mice ($N=8$ mice for vehicle, 11 for AβOs, 11 for exercised, 7 for exercised + AβOs, and 9 for intraperitoneal anti-FNDC5 + exercise + AβOs). $^*P<0.05$; two-sided one-way ANOVA with Holm–Šidák correction. Values are represented by mean ± s.e.m. **i**, APP/PS1 ΔE9 mice (or wild-type littermates) were injected intraperitoneally with anti-FNDC5 (or an irrelevant IgG) and subjected to exercise. NOR memory was assessed 8 days after the first antibody injection and daily exercise session. Effect of anti-FNDC5 on the beneficial actions of exercise in APP/PS1 ΔE9 mice ($N=9$ mice for wild-type, 8 APP/PS1 ΔE9, 7 wild-type intraperitoneal anti-FNDC5, 8 exercise APP/PS1 ΔE9, 7 APP/PS1 ΔE9 exercise injected intraperitoneally with anti-FNDC5). $^*P<0.05$; one-sample *t*-test. Values are represented by mean ± s.e.m.

levels of FNDC5/irisin triggered by AβOs (Fig. 6h). Interestingly, we observed that administration of anti-FNDC5 led to a decrease in hippocampal FNDC5/irisin levels in exercised AβO-infused mice (Fig. 6h). Collectively these results indicate that peripheral irisin may reach the brain and mediate the neuroprotective actions of exercise in synaptic plasticity and memory in AD.

Lastly, we tested whether the approach to neutralize peripheral FNDC5/irisin using an anti-FNDC5 antibody would block the beneficial effects of exercise on memory in APP/PS1 ΔE9 mice. Our results showed that peripheral administration of the anti-FNDC5 antibody prevented the protective actions of exercise in APP/PS1 ΔE9 mice in the NOR test (Fig. 6i). Collectively, these results importantly demonstrate that FNDC5/irisin mediates the positive effects of exercise on synaptic plasticity and memory.

Discussion

AD is a neurological disorder that primarily affects memory, with no cure to date. A variety of potential underlying mechanisms have been proposed to explain the pathogenesis of AD[10,36]. Considerable evidence indicates that memory impairment in AD is caused by synapse failure and loss[2,37,38]. Thus, therapies aimed at restoring or preserving synapse function and cognition are highly warranted.

Irisin was originally discovered as an exercise-induced myokine that shifts the adipose metabolism toward a thermogenic profile[16,39]. There has been some debate as to the nature and identity of FNDC5/irisin, and to its functional relevance in humans[40]. While concerns have been expressed regarding the lack of specificity of anti-irisin antibodies[41], sensitive approaches have been successfully employed to confirm the identity of irisin and to measure its circulating levels in humans[17,20]. Three complementary lines of evidence indicate the specificity of the anti-FNDC5 antibody and ELISA kit used in the current work: (1) FNDC5/irisin levels detected by ELISA showed the expected increase or decrease, respectively, when FNDC5/irisin was overexpressed by use of an adenoviral vector (in both brain and circulation) or when it was knocked down in the brain using a lentiviral vector; (2) surface labeling of FNDC5/irisin by anti-FNDC5 in cultured neurons was predictably reduced in neurons infected by a lentiviral vector harboring shRNA to knock down FNDC5/irisin; (3) mass spectrometry analysis identified peptides contained within FNDC5 in excised gel bands that were immunolabeled by the anti-FNDC5 antibody. By coupling immunodetection and mass spectrometry, we offer initial evidence that FNDC5/irisin is present in multiple forms with distinct apparent molecular weights in the brain, suggesting it may undergo posttranslational modifications and/or exist in different aggregation states. Indeed, putative glycosylation sites are present in FNDC5/irisin[21], and previous reports have suggested that shifts in electrophoretic mobility of FNDC5/irisin are due to glycosylation[16,20].

An interesting study demonstrated that FNDC5/irisin is induced via PGC-1α in the mouse brain and promotes BDNF expression[18]. Extending those previous findings and arguing for a physiological role of FNDC5/irisin in the human brain, we show that ex vivo human adult cortical slices express FNDC5/irisin and respond to exogenous recombinant irisin by activating the cAMP–PKA–CREB memory pathway[42]. Our in vitro findings further show that irisin blocks AβO binding to neurons and prevents AβO-induced eIF2α-P and inhibition of protein synthesis. We and others have recently described these events as essential for synapse and memory failure in AD models, thereby pinpointing a potential downstream pathway by which irisin preserves memory[10,26,30]. We note that the cellular receptor(s) for irisin remain(s) to be identified, which limits current knowledge on downstream signaling mechanisms. The identification of the irisin receptor(s) and the detailed signaling mechanisms triggered in the periphery and in the brain are needed in the field.

The reduced brain and CSF levels of FNDC5/irisin in AD patients and in animal models reported in this study support the notion that defective brain hormonal signaling in AD impacts mechanisms related to memory formation and brain function[3–5]. It is noteworthy that we found a positive correlation between age and CSF irisin in control, non-demented individuals, but not in MCI and AD patients, suggesting that the increase in brain FNDC5/irisin with aging may be part of an endogenous mechanism to cope with the many challenges faced by the aging brain.

Irisin was reduced in the CSF of AD patients, but not in plasma, indicating a specific decrease in the CNS. Our finding that hippocampal FNDC5/irisin is reduced in moderate-to-late AD, but not in MCI, suggests that decreased FNDC5/irisin is not a likely cause of early cognitive impairment in AD, but may contribute to memory

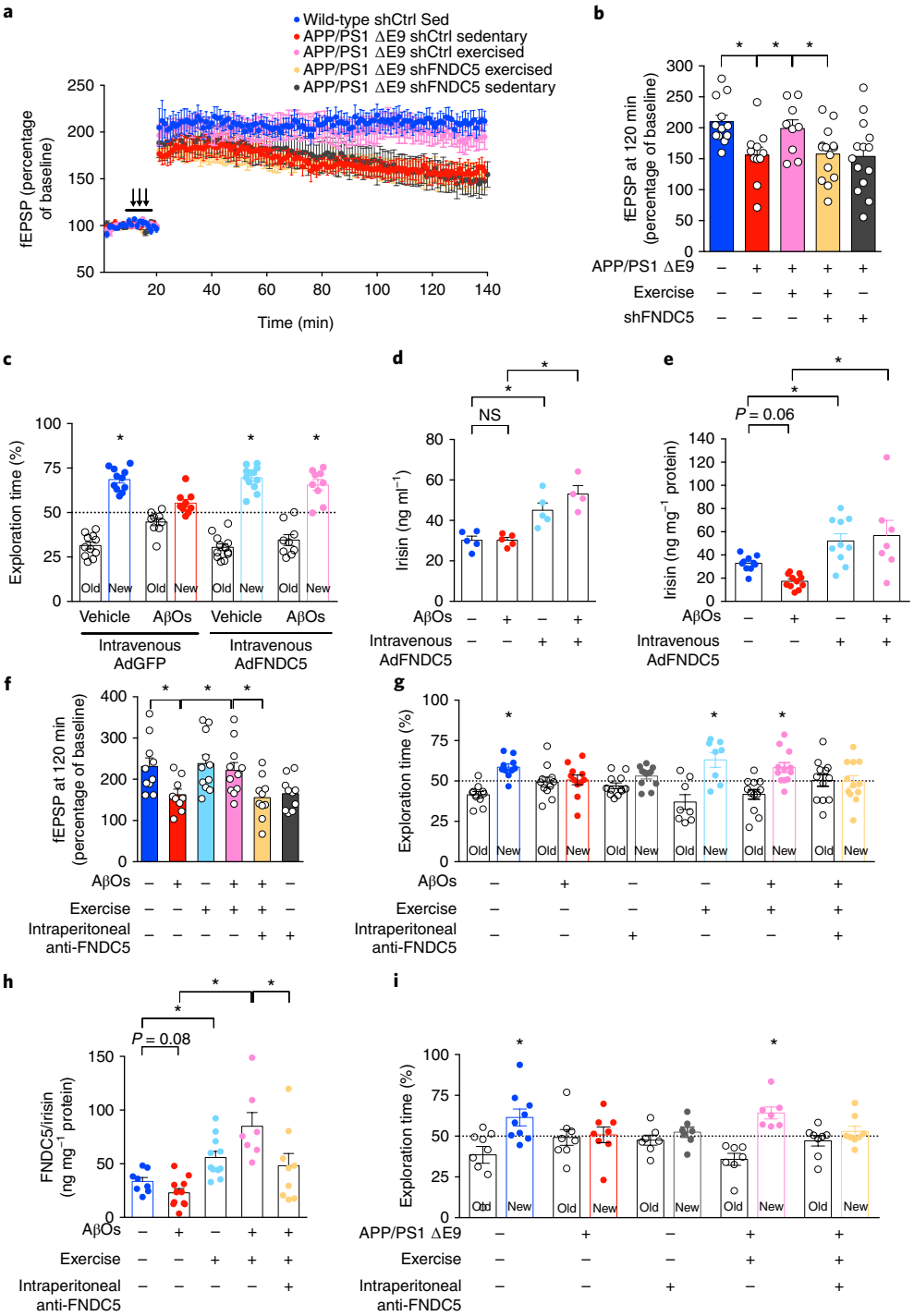

defects as disease progresses. Additional studies measuring irisin levels in the CSF during healthy aging and in patients with other neurological disorders are anticipated and will help to determine when irisin levels decrease during the course of AD.

Blockade of either brain or peripheral FNDC5/irisin in mice impaired LTP and NOR memory, implicating FNDC5/irisin in physiological memory processes. However, future studies are warranted to address the precise physiological roles of brain and peripheral FNDC5/irisin in the formation and consolidation of different types of memories.

It is noteworthy that peripheral administration of AdFNDC5 led to increases in hippocampal FNDC5/irisin and protected mice against memory impairment induced by AβOs. Most importantly, peripheral FNDC5/irisin is implicated in the preservation of hippocampal FNDC5/irisin levels, synaptic plasticity, and memory in AD mice. Collectively, these results provide mechanistic information on the beneficial actions of FNDC5/irisin in the brain and suggest that a cross talk between peripheral and central FNDC5/irisin influences synaptic plasticity and memory in mice.

Physical exercise has been previously shown to induce memory-related events in the brain[43–45] and has been proposed as an approach to reduce the risk of AD, potentially bringing about significant benefits to subjects with MCI and early AD[46–49]. Many efforts to identify the endogenous molecules responsible for the beneficial effects of exercise are underway. Brain PGC-1α and BDNF[28,50], as well as peripheral cathepsin B and β-hydroxybutyrate[51,52], have been

described as important molecules acting as mediators of exercise-induced neuroprotection. The results presented in this study add FNDC5/irisin to this list.

Our findings suggest that FNDC5/irisin could comprise an attractive novel therapy aimed to prevent dementia in patients at risk, as well as delay its progression in patients at the later stages, including those who can no longer exercise. Many patients with dementia are disabled due to other age-related conditions or comorbidities (for example, arthritis, heart disease, obesity, visual problems, depression) that preclude them from engaging in regular physical exercise. Therefore, the development of alternative approaches that build on the beneficial effects of exercise in the brain may benefit those patients.

In conclusion, our results demonstrate that FNDC5/irisin levels are reduced in human AD brains and CSF and in AD mouse models, and that boosting either brain or peripheral FNDC5/irisin levels attenuates synaptic and memory impairments in AD mouse models. We further show that FNDC5/irisin is a novel mediator of the beneficial effects of exercise on synapse function and memory in AD models. Bolstering brain FNDC5/irisin levels, either pharmacologically or through exercise, may thus constitute a novel therapeutic strategy to protect and/or repair synapse function and prevent cognitive decline in AD.

Online content

Any methods, additional references, Nature Research reporting summaries, source data, statements of data availability and associated accession codes are available at https://doi.org/10.1038/s41591-018-0275-4.

Received: 13 October 2016; Accepted: 2 November 2018;
Published online: 7 January 2019

References

1. Prince, M. et al. The global prevalence of dementia: a systematic review and metaanalysis. *Alzheimers Dement.* **9**, 63–75.e62 (2013).
2. Ferreira, S. T., Lourenco, M. V., Oliveira, M. M. & De Felice, F. G. Soluble amyloid-β oligomers as synaptotoxins leading to cognitive impairment in Alzheimer's disease. *Front. Cell. Neurosci.* **9**, 191 (2015).
3. Fernandez, A. M. & Torres-Alemán, I. The many faces of insulin-like peptide signalling in the brain. *Nat. Rev. Neurosci.* **13**, 225–239 (2012).
4. Biessels, G. J. & Reagan, L. P. Hippocampal insulin resistance and cognitive dysfunction. *Nat. Rev. Neurosci.* **16**, 660–671 (2015).
5. McEwen, B. S. Preserving neuroplasticity: role of glucocorticoids and neurotrophins via phosphorylation. *Proc. Natl Acad. Sci. USA* **112**, 15544–15545 (2015).
6. During, M. J. et al. Glucagon-like peptide-1 receptor is involved in learning and neuroprotection. *Nat. Med.* **9**, 1173–1179 (2003).
7. Chiu, S.-L., Chen, C.-M. & Cline, H. T. Insulin receptor signaling regulates synapse number, dendritic plasticity, and circuit function in vivo. *Neuron* **58**, 708–719 (2008).
8. Grillo, C. A. et al. Hippocampal insulin resistance impairs spatial learning and synaptic plasticity. *Diabetes* **64**, 3927–3936 (2015).
9. Irving, A. J. & Harvey, J. Leptin regulation of hippocampal synaptic function in health and disease. *Philos. Trans. R. Soc. Lond. B* **369**, 20130155 (2013).
10. Lourenco, M. V., Ferreira, S. T. & De Felice, F. G. Neuronal stress signaling and eIF2α phosphorylation as molecular links between Alzheimer's disease and diabetes. *Prog. Neurobiol.* **129**, 37–57 (2015).
11. Bomfim, T. R. et al. An anti-diabetes agent protects the mouse brain from defective insulin signaling caused by Alzheimer's disease-associated Aβ oligomers. *J. Clin. Invest.* **122**, 1339–1353 (2012).
12. Talbot, K. et al. Demonstrated brain insulin resistance in Alzheimer's disease patients is associated with IGF-1 resistance, IRS-1 dysregulation, and cognitive decline. *J. Clin. Invest.* **122**, 1316–1338 (2012).
13. De Felice, F. G., Lourenco, M. V. & Ferreira, S. T. How does brain insulin resistance develop in Alzheimer's disease? *Alzheimers Dement.* **10**, S26–S32 (2014).
14. Wadman, M. US government sets out Alzheimer's plan. *Nature* **485**, 426–427 (2012).
15. De Felice, F. G. Alzheimer's disease and insulin resistance: translating basic science into clinical applications. *J. Clin. Invest.* **123**, 531–539 (2013).
16. Boström, P. et al. A PGC1-α-dependent myokine that drives brown-fat-like development of white fat and thermogenesis. *Nature* **481**, 463–468 (2012).
17. Jedrychowski, M. P. et al. Detection and quantitation of circulating human irisin by tandem mass spectrometry. *Cell Metab.* **22**, 734–740 (2015).
18. Wrann, C.D. et al. Exercise induces hippocampal BDNF through a PGC-1α/FNDC5 pathway. *Cell Metab.* **18**, 649–659 (2013).
19. Chen, K. et al. Irisin protects mitochondria function during pulmonary ischemia/reperfusion injury. *Sci. Transl. Med.* **9**, eaao6298 (2017).
20. Lee, P. et al. Irisin and FGF21 are cold-induced endocrine activators of brown fat function in humans. *Cell Metab.* **19**, 302–309 (2014).
21. Schumacher, M. A., Chinnam, N., Ohashi, T., Shah, R. S. & Erickson, H. P. The structure of irisin reveals a novel intersubunit β-sheet fibronectin type III (FNIII) dimer: implications for receptor activation. *J. Biol. Chem.* **288**, 33738–33744 (2013).
22. Mucke, L. & Selkoe, D. J. Neurotoxicity of amyloid β-protein: synaptic and network dysfunction. *Cold Spring Harb. Perspect. Med.* **2**, a0063381 (2012).
23. Sebollela, A. et al. Amyloid-β oligomers induce differential gene expression in adult human brain slices. *J. Biol. Chem.* **287**, 7436–7445 (2012).
24. Colaianni, G. et al. The myokine irisin increases cortical bone mass. *Proc. Natl Acad. Sci. USA* **112**, 12157–12162 (2015).
25. Figueiredo, C. P. et al. Memantine rescues transient cognitive impairment caused by high-molecular-weight Aβ oligomers but not the persistent impairment induced by low-molecular-weight oligomers. *J. Neurosci.* **33**, 9626–9634 (2013).
26. Lourenco, M. V. et al. TNF-α mediates PKR-dependent memory impairment and brain IRS-1 inhibition induced by Alzheimer's β-amyloid oligomers in mice and monkeys. *Cell Metab.* **18**, 831–843 (2013).
27. Jankowsky, J. L. et al. Co-expression of multiple transgenes in mouse CNS: a comparison of strategies. *Biomol. Eng.* **17**, 157–165 (2001).
28. Cheng, A. et al. Involvement of PGC-1α in the formation and maintenance of neuronal dendritic spines. *Nat. Commun.* **3**, 1250 (2012).
29. Holcomb, L. et al. Accelerated Alzheimer-type phenotype in transgenic mice carrying both mutant amyloid precursor protein and presenilin 1 transgenes. *Nat. Med.* **4**, 97–100 (1998).
30. Ma, T. et al. Suppression of eIF2α kinases alleviates Alzheimer's disease-related plasticity and memory deficits. *Nat. Neurosci.* **16**, 1299–1305 (2013).
31. Yang, W. et al. Repression of the eIF2α kinase PERK alleviates mGluR-LTD impairments in a mouse model of Alzheimer's disease. *Neurobiol. Aging* **41**, 19–24 (2016).
32. Trinh, M. A. & Klann, E. Translational control by eIF2α kinases in long-lasting synaptic plasticity and long-term memory. *Neurobiol. Learn. Mem.* **105**, 93–99 (2013).
33. Gong, B. et al. Persistent improvement in synaptic and cognitive functions in an Alzheimer mouse model after rolipram treatment. *J. Clin. Invest.* **114**, 1624–1634 (2004).
34. Vitolo, O. V. et al. Amyloid β-peptide inhibition of the PKA/CREB pathway and long-term potentiation: reversibility by drugs that enhance cAMP signaling. *Proc. Natl Acad. Sci. USA* **99**, 13217–13221 (2002).
35. Schaefer, N. et al. The malleable brain: plasticity of neural circuits and behavior: a review from students to students. *J. Neurochem.* **142**, 790–811 (2017).
36. Katsnelson, A., De Strooper, B. & Zoghbi, H. Y. Neurodegeneration: from cellular concepts to clinical applications. *Sci. Transl. Med.* **8**, 364ps318 (2016).
37. Selkoe, D. J. Alzheimer's disease is a synaptic failure. *Science* **298**, 789–791 (2002).
38. Lepeta, K. et al. Synaptopathies: synaptic dysfunction in neurological disorders: a review from students to students. *J. Neurochem.* **138**, 785–805 (2016).
39. Zhang, Y. et al. Irisin stimulates browning of white adipocytes through mitogen-activated protein kinase p38 MAP kinase and ERK MAP kinase signaling. *Diabetes* **63**, 514–525 (2014).
40. Timmons, J. A., Baar, K., Davidsen, P. K. & Atherton, P. J. Is irisin a human exercise gene? *Nature* **488**, E9–E10 (2012).
41. Albrecht, E. et al. Irisin: a myth rather than an exercise-inducible myokine. *Sci. Rep.* **5**, 8889 (2015).
42. Martin, K. C. & Kandel, E. R. Cell adhesion molecules, CREB, and the formation of new synaptic connections. *Neuron* **17**, 567–570 (1996).
43. Suwabe, K. et al. Rapid stimulation of human dentate gyrus function with acute mild exercise. *Proc. Natl Acad. Sci. USA* **115**, 10487–10492 (2018).
44. van Praag, H., Fleshner, M., Schwartz, M. W. & Mattson, M. P. Exercise, energy intake, glucose homeostasis, and the brain. *J. Neurosci.* **34**, 15139–15149 (2014).
45. Neufer, P. D. et al. Understanding the cellular and molecular mechanisms of physical activity-induced health benefits. *Cell Metab.* **22**, 4–11 (2015).
46. Baker, L. D. et al. Effects of aerobic exercise on mild cognitive impairment: a controlled trial. *Arch. Neurol.* **67**, 71–79 (2010).
47. Buchman, A. S. et al. Total daily physical activity and the risk of AD and cognitive decline in older adults. *Neurology* **78**, 1323–1329 (2012).

48. Okonkwo, O. C. et al. Physical activity attenuates age-related biomarker alterations in preclinical AD. *Neurology* **83**, 1753–1760 (2014).
49. Müller, S. Relationship between physical activity, cognition, and Alzheimer pathology in autosomal dominant Alzheimer's disease. *Alzheimers Dement.* **14**, 1427–1437 (2018).
50. Mattson, M. P. Energy intake and exercise as determinants of brain health and vulnerability to injury and disease. *Cell Metab.* **16**, 706–722 (2012).
51. Moon, H. Y. et al. Running-induced systemic cathepsin B secretion is associated with memory function. *Cell Metab.* **24**, 332–340 (2016).
52. Sleiman, S. F. et al. Exercise promotes the expression of brain derived neurotrophic factor (BDNF) through the action of the ketone body β-hydroxybutyrate. *eLife* **5**, e15092 (2016).

Acknowledgements

This work was supported by grants from Alzheimer Society of Canada (to F.G.D.F.) and the Weston Brain Institute (to F.G.D.F.), National Institute for Translational Neuroscience (INNT/Brazil) (465346/2014-6 to S.T.F. and F.G.F.), Human Frontier Science Program (to F.G.D.F.), International Society for Neurochemistry (CAEN 1B to M.V.L.), National Institutes of Health (NIH-R01NS049442 to O.A.), Canadian Institutes of Health Research (CIHR MOP 136940 and MOP 89919 to V.F.P. and M.A.M.P.), and from the Brazilian funding agencies Conselho Nacional de Desenvolvimento Científico e Tecnológico (CNPq) (451195/2017-5 to M.V.L., 406436/2016-9 to S.T.F., and 473324/2013-0 to F.G.D.F.) and Fundação Carlos Chagas Filho de Amparo à Pesquisa do Estado do Rio de Janeiro (FAPERJ) (202.817/2016 to M.V.L., 201.432/2014 to S.T.F., and 202.944/2015 to F.G.D.F.). R.L.F, G.B.d.F., G.C.K., F.C.R., J.R.C., D.B., and L.F.-G. were supported by fellowships granted by FAPERJ, CNPq, or Comissão de Aperfeiçoamento de Pessoal de Nível Superior (CAPES/Brazil; financial code 001). S.M. was supported by an NIH T32 grant (AG057461). We acknowledge the University of Kentucky Alzheimer's Disease Center and its Neuropathology Core, which is supported by NIH/NIA P30 AG028383, for brain samples. We thank W.L. Klein (Northwestern University) for the kind gift of oligomer-specific NU4 antibodies, B.M. Spiegelman (Harvard University) for sharing AdGFP and AdFNDC5 adenoviral constructs, and J. Wang (Queen's University, Canada) for help with mass spectrometry analyses. We also thank A. Lepelley, M. Oliveira, M. Melo, A.C. Rangel, and the CENABIO team for technical and/or administrative assistance.

Author contributions

M.V.L., R.L.F., O.A., S.T.F., and F.G.D.F. designed the study. M.V.L., R.L.F., G.B.d.F., H.Z., G.C.K, F.C.R., R.A.G., J.R.C., D.B., A.S., H.B., L.A.G., L.F.-G., S.M., and J.F.A. performed the research. M.V.L., R.L.F., G.B.d.F., H.Z., D.B., A.S., S.M., J.F.A., O.A., S.T.F., and F.G.D.F. analyzed the data. J.F.A., D.M.W., J.M.d.S., S.A.-L., V.F.P., M.A.M.P., F.T.-M., P.M., and O.A. contributed the reagents, materials, and analysis tools. M.V.L., R.L.F., G.B.d.F., A.S, J.F.A., F.T-M., P.M., O.A., S.T.F., and F.G.D.F. analyzed and discussed the results. M.V.L., R.L.F., S.T.F., and F.G.D.F. wrote the manuscript.

Competing interests

The authors declare no competing interests.

Additional information

Extended data is available for this paper at https://doi.org/10.1038/s41591-018-0275-4.

Supplementary information is available for this paper at https://doi.org/10.1038/s41591-018-0275-4.

Reprints and permissions information is available at www.nature.com/reprints.

Correspondence and requests for materials should be addressed to O.A. or S.T.F. or F.G.D.F.

Publisher's note: Springer Nature remains neutral with regard to jurisdictional claims in published maps and institutional affiliations.

© The Author(s), under exclusive licence to Springer Nature America, Inc. 2019

Methods

Reagents. $A\beta_{1-42}$ was obtained from American Peptide Company or AnaSpec; 1,1,1,3,3,3-hexafluoro-2-propanol (HFIP), dimethyl sulfoxide (DMSO), anti-ATF4 antibody (no. WH0000468M1), myristoylated PKI 14–22, and poly-L-lysine were obtained from Sigma-Aldrich. Culture media, qPCR kits, Alexa-labeled phalloidin, fluorescent secondary antibodies for immunocytochemistry, ProLong antifade mountant with 4,6-diamidino-2-phenylindole (DAPI) were obtained from Thermo Fisher Scientific. IRDye-conjugated antibodies for immunoblotting were obtained from LI-COR. Electrophoresis gels and reagents were obtained from Bio-Rad Laboratories. SuperSignal chemiluminescence reagents and bicinchoninic acid assay kit were obtained from Pierce. Anti-eIF2α-P (phosphoS51) (no. BML-SA405-100), anti-eIF2α (total) (no. ADI-KAP-CP130), and PKA activity kits were obtained from Enzo Life Sciences. The antibody against puromycin (clone 12D10) (no. MABE343) was obtained from Merck Millipore. The antibody against β-tubulin III (Tuj1) (no. MAB1195) was obtained from R&D Systems. ELISA kits for BDNF and phosphorylated CREB (pCREB), and antibodies against FNDC5 (no. ab131390), GAPDH (no. ab9485), and β-actin (no. ab8226) were obtained from Abcam. The antibody against BDNF (no. sc546) was obtained from Santa Cruz Biotechnology. The Aβ oligomer-sensitive antibody NU4 was a kind gift from Dr. William L. Klein (Northwestern University). Recombinant irisin expressed in CHO cells was from AdipoGen Life Sciences. Irisin ELISA kits were obtained from Phoenix Pharmaceuticals. cAMP ELISA kits were from R&D Systems. The mouse synaptic plasticity PCR array kit (no. PAM126Z) was obtained from QIAGEN. Adenoviral vectors designed to express GFP or FNDC5 (AdGFP or AdFNDC5, respectively) were produced by ViraQuest Inc. using the Gateway expression system (Thermo Fisher Scientific), as described previously[16,18], and were kindly donated by Dr. Bruce Spiegelman (Harvard University). High-titer viral particles (1.0×10^{11} per ml) were diluted and used in the reported experiments. MISSION lentiviral particles targeting luciferase (control) or FNDC5 were obtained from Sigma-Aldrich.

Nano-liquid chromatography (nano-LC)-linear trap quadropole Orbitrap mass spectrometry analysis of immunodetected FNDC5/irisin in mouse hippocampus. Mouse hippocampal homogenates (50 µg per lane) were resolved in 10% SDS–polyacrylamide gel electrophoresis (PAGE) gels followed by electrotransfer of half of the gel (first 6 lanes) onto nitrocellulose membranes at 4 °C, constant 100 V for 90 min in Tris-glycine transfer buffer (Bio-Rad Laboratories, catalog no.1610734) containing 20% (v/v) methanol. Blots were blocked in membrane blocking solution (Thermo Fisher Scientific, catalog no. 000105) for 1 h at room temperature, incubated overnight at 4 °C with anti-FNDC5 polyclonal antibody (1:1,000 dilution in blocking buffer; Abcam), washed 3 times for 10 minutes with tris-buffered saline and Tween (TBST), incubated for 1 h at room temperature with peroxidase-conjugated goat anti-rabbit immunoglobulin G (IgG) secondary antibody (1:50,000 dilution in blocking buffer; Thermo Fisher Scientific), developed using Pierce ECL Western Blotting Substrate (Thermo Fisher Scientific) and imaged on a Azure c600 (Azure Biosystems) imaging station. The positions of immunolabeled bands in the membranes were used to guide excision of the corresponding bands from unstained separate lanes from the other half of the gel (mirror) that had not been electrotransferred. Excised gel bands were subjected to in-gel digestion as described previously[53]. Commercial recombinant irisin expressed in CHO cells (AdipoGen, catalog no. AG-40B-0136) digested in aqueous solution or digested/eluted from bands excised from an SDS–PAGE gel (run exactly as described earlier) were used as standards.

Mass spectrometry analyses were carried out at the Queen's University Mass Spectrometry facility in Kingston, Canada. Samples containing tryptic fragments were analyzed on an Orbitrap Velos Pro (Thermo Fisher Scientific) mass spectrometer coupled to a nano-LC system and nano-electrospray ionization source (Thermo Fischer Scientific). Eluent A was aqueous formic acid (0.1%, v/v) and eluent B was high-performance liquid chromatography-grade acetonitrile containing 0.1% (v/v) formic acid. Samples (10 µl) were injected by the autosampler onto the trap column (C18, internal diameter 100 µm, length 20 mm, particle diameter 5 µm) (CMP Scientific) and were separated on an analysis column (C18, internal diameter 75 µm, length 100 mm, particle diameter 5 µm) (CMP Scientific) at a flow rate of 30 nl min^{-1} using two step gradients, from 5 to 50% eluent B over 70 min to 100% eluent B over 45 min, followed by 100% eluent B for 15 min. The transfer capillary temperature was set to 270 °C. An ion spray voltage of 2.0 kV was applied to a PicoTip on-line nano-electrospray ionization emitter (New Objective). Mass spectrometry scans were acquired at an Orbitrap resolution of 60,000 for an *m/z* range from 150 to 2,000. Following data acquisition, tandem mass spectrometry spectra were analyzed with Proteome Discoverer 1.4 (Thermo Fischer Scientific) with a precursor mass tolerance of 10 parts per million (ppm) and fragment mass tolerance of 0.8 Da. Alternatively, we manually searched for tandem mass spectrometry spectra corresponding to specific *m/z* values for peptides identified in recombinant irisin standards in the raw data for samples corresponding to each band excised from the SDS–PAGE gel.

Ex vivo human cortical slices. Adult human cortical slices were previously characterized and prepared as described previously[23,54] with minor modifications. Healthy cortical tissue was obtained from patients with drug-resistant temporal lobe epilepsy subjected to surgical interventions for removal of epileptic foci. Donors were two men (aged 37 and 49) and three women (aged 18, 39, and 66). After dissection under sterile conditions, 400-µm-thick slices were prepared using a McIlwain tissue chopper and plated on Neurobasal-A medium containing 2% B27, 500 µM glutamine, 5 ng ml^{-1} FGF2, 2 µM dehydroepiandrosterone sulfate, 1 ng ml^{-1} BDNF and 50 µg ml^{-1} gentamicin. After 7 days in culture at 37 °C and 5% CO_2, slices were exposed to AβOs (500 nM) or the corresponding volume of vehicle for 12 h and were processed for biochemical analyses thereafter. When present, irisin (25 nM) was added for the indicated time periods and tissue was harvested for subsequent analyses.

Postmortem human brain tissue. For western blotting analyses, brain samples from noncognitively impaired, early or late AD patients (defined by combined pathological and cognitive assessment) were obtained from the University of Kentucky Alzheimer's Disease Center Biobank. Experimental procedures involving human tissue were in compliance with the University of Kentucky Institutional Review Board (IRB). Samples from Brodmann areas 21/22 (superior and mid-temporal gyri) were snap frozen at autopsy as previously described. AD tissue was from symptomatic individuals with clinical and pathological features, which are described in Supplementary Table 1. All patients were categorized by Mini–Mental State Examination as control (26–30), early AD (20–25), and late AD (13–17). Sample groups were separated so as to clearly define differences in content of proteins of interest and Mini–Mental State Examination score.

Human CSF and plasma. CSF or plasma from control and AD patients were collected after extensive neuropsychological investigation supervised by a board-certified psychiatrist, as described previously[55]. The study cohort included men and women. Age (mean ± s.d.), in years, was distributed as follows: controls (67.5 ± 4.9); MCI (71.5 ± 5.8); AD (72.5 ± 8.1); and LBD (71.6 ± 7.0). CSF was collected by lumbar puncture performed at 9 a.m. in all cases. CSF was centrifuged, aliquoted, and immediately frozen at −80 °C. Total blood was collected in heparin-coated tubes and plasma was isolated by centrifugation. Irisin concentration was determined using a commercial ELISA kit (Phoenix Pharmaceuticals), according to the manufacturer's instructions.

Animals. Male C57BL/6 or Swiss mice were obtained from the animal facility at the Federal University of Rio de Janeiro and were 2.5–3 months old at the beginning of experiments. Male and female APP/PS1 ΔE9 mice on a C57BL/6 background[27] were originally obtained from The Jackson Laboratories and bred at our animal facility. Male and female double transgenic mice (APP/PS1 M146L) were obtained by crossing Tg2576 mice harboring mutant human APP (K670M:N671L) with mutant PS1 (M146L) mice[29]. Wild-type littermates were used as controls. All animals had their genotypes confirmed before use. Animals were housed in groups of five per cage with free access to food and water, under a 12 h light–dark cycle, with controlled room temperature and humidity. Experiments using C57BL/6 mice are presented in the main text, while biochemical and behavioral experiments in Swiss mice performed to validate and confirm our findings are presented as Extended Data Figures. All procedures followed the *Principles of Laboratory Animal Care* formulated by the US National Institutes of Health.

Brain infusions in mice. For intracerebroventricular infusion of AβOs, mice were anesthetized with 2.5% isoflurane (Cristália) using a vaporizer system (Norwell) and were gently restrained only during the injection procedure, as described previously[25,56]. A 2.5-mm-long needle was unilaterally inserted 1 mm to the right of the midline point equidistant from each eye and 1 mm posterior to a line drawn through the anterior base of the eye[25,26,56,57]; 10 pmol AβOs (or vehicle) was injected in a final volume of 3 µl and the needle was kept in place for an additional 30 s to prevent backflow. Mice that showed signs of misplaced injections or any sign of hemorrhage were excluded from further analysis. Recombinant irisin (75 pmol per site) was bilaterally delivered into the hippocampal CA1 region (stereotaxical coordinates relative to bregma: 2.0 mm anteroposterior, ±1.5 mm mediolateral, 1.5 mm dorsoventral), immediately before AβO injections. Adenoviral particles (1×10^8) harboring GFP (AdGFP) or FNDC5 (AdFNDC5) constructs were stereotaxically injected into the right lateral ventricle of wild-type C57BL/6 or APP/PS1 mice (coordinates relative to bregma: 0.2 mm anteroposterior; 1.0 mediolateral; 2.4 mm dorsoventral). Injections were performed in a volume of 2 µl infused over 30 s. Behavioral studies were carried out at least 6 days post-injection. Lentiviral particles expressing shRNA against murine FNDC5 or luciferase (control) were injected intracerebroventricularly as described earlier. Lentiviruses (titer of $1.0–2.0\times10^9$ particles per ml) were injected in a volume of 3 µl per animal. Behavioral and electrophysiological studies were carried out four weeks post-injections. Six days before the AβO infusions, AdFNDC5 or AdGFP (100 µl; 10^6 particles per µl) were injected intravenously into the caudal vein in mice anesthetized with isoflurane (2.5%) and gently restrained during the procedure.

Aerobic exercise in mice. Swiss mice were adapted to swimming for 10 min each day for 2 days to reduce water-induced stress. The duration of exercise was gradually increased until mice swam for 60 min, which was reached, on average,

on the fifth day of training. Exercise sessions were performed during the light cycle and consisted of 60 min swimming sessions, 5 days per week for 5 weeks. Mice swam in groups of four in plastic barrels (60 cm depth × 45 cm diameter). Water temperature was maintained at ~24 °C. On the fifth week of training, animals were injected intracerebroventricularly with AβOs (10 pmol) and the NOR task was performed 24 h or 5 days post-injection of AβOs. CFC was performed 6–7 days post-injection. Animals were killed by decapitation 1 h after the last test session. Since C57BL/6 are smaller than Swiss mice and less resistant to long exercise sessions, we adapted the protocol when using C57BL/6 mice. In a set of experiments, wild-type or APP/PS1 ΔE9 mice on a C57BL/6 background swam for 20 min for 3 weeks in groups of 4 before LTP recordings. In some experiments, wild-type C57BL/6 mice underwent exercise and were injected intraperitoneally with anti-FNDC5 antibody or control IgG (5 µg) after the last two exercise sessions, and/or were infused intracerebroventricularly with AβOs (10 pmol) in the last exercise session. Mice were assessed in the NOR test 24 h after oligomer injections. Alternatively, in experiments aimed at testing NOR memory, wild-type or APP/PS1 ΔE9 mice were subjected to daily swimming sessions for 1 week, and were injected intraperitoneally with anti-FNDC5 antibody or nonspecific IgG (5 µg) on the first, fourth, and seventh day. NOR was performed 24 h after the last exercise session.

Behavioral testing. *NOR.* Object recognition tests were carried out in an open field arena measuring 0.3 × 0.3 × 0.45 m^3, as described previously[25,26]. Total distance and velocity during the 5-minute open field session were recorded as measures of locomotor activity; no differences were found among the groups. Animals were trained in a 5-min-long session during which they were placed at the center of the arena in the presence of two identical objects. Exploratory behavior (amount of time exploring each object) was recorded by trained researchers. One hour after training, animals were reinserted into the arena for the test session, in which one of the objects had been replaced by a different (novel) object. Again, the amount of time spent exploring familiar and novel objects was measured. Animals that had a total exploration time below 8 s were excluded from the NOR tests. Results are expressed as the percentage of time exploring each object during the training or test session, and were analyzed using a one-sample Student's *t*-test comparing the mean exploration time for each object with the fixed value of 50% (chance level).

CFC. CFC was evaluated as described previously[26,58]. For experiments in APP/PS1 mice, animals were allowed to freely explore the conditioning chamber (0.4 × 0.25 × 0.3 m^3) for 2 min, after which a 2-s shock stimulus (0.8 mA) was applied to the floor. Animals remained in the cage for an additional 1 min. After 24 h, mice were placed in the same cage and allowed to explore it for 5 min in the absence of an electric shock. Freezing events were recorded during this period; the percentage of time in freezing behavior was calculated for each animal using the Ethovision software (Noldus Information Technology). In experiments with AβO-injected mice and corresponding controls, animals were allowed to freely explore the training chamber (0.25 × 0.25 × 0.25 m^3; Harvard Apparatus) for 3 min, after which they received two 2-s-long 0.35 mA foot shocks with a 30 s interval. Animals were removed from the cage after 30 s. Twenty-four hours thereafter, they were reinserted into the box for 5 min and the total freezing time during the test session was determined. The statistical significance of differences between groups was evaluated using a two-way ANOVA followed by Holm–Šidák post-hoc test. After completion of the fear conditioning experiments, animals were subjected to sensory threshold assessment to investigate potentially different susceptibilities to shock; no significant differences in sensory response were found among experimental groups.

Two-day RAWM. RAWM was performed in APP/PS1 mice as described previously[59]. Briefly, mice were tested for their ability to find a platform located in a defined arm of a 6-arm maze along 30 trials in 2 days. On day 1, five training blocks were performed with alternation between visible and hidden platform. On day 2, all five blocks had the platform hidden. A training block comprises 3 trials of 60 s each. The number of entries into incorrect maze arms (errors) was recorded for each session and the number of errors per block was averaged. Visual and motor abilities were assessed by recording swimming velocity and latency to reach a visible platform in an open swimming pool task. Animal tracking in visible platform experiments was automatically performed with the Ethovision software.

Open field. Control experiments to assess locomotor and exploratory activity were performed in the same boxes as the NOR experiments, in which mice were allowed to freely move for 5 min. Total distance, mean velocity, and percentage of time in the center or periphery were recorded and quantified using the ANY-maze software (Stoelting Co.).

LTP measurements. Mice were killed by cervical dislocation followed by decapitation; their hippocampi were immediately removed. Transverse hippocampal slices (400 µm) were cut, placed on infusion chambers on artificial CSF (aCSF; 124 mM NaCl, 4.4 mM KCl, 1 mM Na_2HPO_4, 25 mM $NaHCO_3$, 2 mM $MgCl_2$, 2 mM $CaCl_2$, 10 mM glucose) and allowed to recover for 90–120 min. For experiments with recombinant irisin and/or AβOs in slices from wild-type mice, AβOs (200 nM) and/or recombinant irisin (25 nM) were diluted in aCSF and perfused for 20 min before stimulus. For experiments with exercised mice that received anti-FNDC5 (or control IgG), animals were exercised for three sessions and received an intraperitoneal injection of anti-FNDC5 antibody (or nonspecific IgG) after each session. An additional anti-FNDC5 injection was performed before slice preparation and perfusion with AβOs or vehicle. For experiments with adenovirus-mediated FNDC5 expression, wild-type or APP/PS1 ΔE9 mice were injected intracerebroventricularly with AdGFP (control) or AdFNDC5 14 days before being killed and slice preparation. Field EPSPs were recorded from the hippocampal CA1 region according to established procedures[34,60].

AβOs. Oligomers were prepared from synthetic $Aβ_{1–42}$ and were routinely characterized by size-exclusion chromatography, as described previously[23,25,61,62]. For the electrophysiology experiments in hippocampal slices, oligomers were prepared as previously reported[60,63] and perfused at a final concentration of 200 nM in aCSF.

Mature hippocampal cultures. Primary rat hippocampal neuronal cultures were maintained in Neurobasal medium supplemented with B27 (Thermo Fisher Scientific), glutamine, and antibiotics according to established procedures[11,26,64], and were used after 18–21 days in vitro. Cultures were exposed to 500 nM AβOs or an equivalent volume of vehicle (2% DMSO in PBS) for the time intervals indicated in each experiment. When present, lentiviral vectors targeting FNDC5 (10^6 ml^{-1}) were allowed to express for 5 days before cells were processed for immunocytochemistry. When present, recombinant irisin (25 nM) or forskolin (10 µM) was added to cultures 15 min before AβOs, and myristoylated PKI 14–22 (1 µM) was added 40 min before irisin.

Immunofluorescence. Cells were fixed in ice-cold 4% formaldehyde plus 4% sucrose for 10 min. AβO-sensitive (NU4 monoclonal antibody[65]) and FNDC5 immunolabeling were performed under non-permeabilizing conditions, while cells labeled for eIF2α-P (1:400), total eIF2α (1:400), GFAP (1:500), βIII-tubulin (1:500), or ATF4 (1:400) were permeabilized in 0.1% Triton X-100 for 5 min before primary antibody incubation, followed by Alexa-conjugated secondary antibodies (Thermo Fisher Scientific). Nuclei were counterstained in DAPI-containing ProLong antifade mounting solution. Coverslips were imaged on a ZEISS AxioObserver Z1 microscope. FNDC5, eIF2α-P, total eIF2α, and ATF4 immunofluorescence intensities were each analyzed in at least 3 experiments (see figure legends) using independent neuronal cultures and AβO preparations. In each experiment, 20–30 images (from 2–3 coverslips) were acquired from each experimental condition. Histogram analysis of fluorescence at each pixel across the images was performed using Image J (National Institutes of Health)[66], as described previously[26]. When indicated, cell bodies were digitally removed from the images so that only immunostaining on dendritic processes was quantified. The statistical significance of differences between experimental groups was assessed with an ANOVA followed by a post-hoc Holm–Šidák test; *P* values are indicated in the figure legends.

Spine density. After treatments, hippocampal neuronal cultures were fixed in ice-cold 4% formaldehyde plus 4% sucrose for 10 min and permeabilized in 0.1% Triton X-100 for 5 min. Cells were then blocked in 3% bovine serum albumin (BSA) for 1 h and stained with Alexa-conjugated phalloidin (2 U per coverslip), which labels F-actin, in 3% BSA for 2 h at room temperature. Coverslips were mounted in DAPI-containing ProLong Gold antifade mountant and stored in a dark and humid chamber overnight. Coverslips were imaged on a ZEISS AxioObserver Z1 microscope. Images were obtained from at least two coverslips per experimental condition for each experiment (three experiments with independent neuronal cultures). Two or three distal dendrite segments were isolated per neuron, and a researcher blind to experimental conditions manually determined the number of spines. Results are expressed as the mean number of spines per µm.

RNA extraction and quantitative RT–PCR. Total RNA was extracted from cultures or animal tissues using SV Total RNA Isolation System (Promega), following the manufacturer's instructions. The purity and integrity of RNA preparations were checked using the 260/280 nm absorbance ratio. Only preparations with 260/280 nm absorbance ratios higher than 1.8 and no signs of RNA degradation were used. RNA concentrations were determined by absorption at 260 nm. For real-time quantitative reverse transcription PCR (qRT–PCR), 1 µg of total RNA was used for complementary DNA (cDNA) synthesis using the High Capacity cDNA Reverse Transcription kit (Thermo Fisher Scientific). Quantitative expression analysis of target genes was performed on a 7500 Fast Real-Time PCR system (Thermo Fisher Scientific) with the *Power* SYBR Green PCR Master Mix. β-Actin (*actb*) was used as an endogenous reference gene for data normalization. qRT–PCR was performed in 20 µl reaction volumes according to the manufacturer's protocols. Primer sequences are described in Supplementary Table 2. Cycle threshold (C_T) values were used to calculate fold changes in gene expression using the $2^{-\Delta\Delta C}{}_T$method[67]. The statistical significance of changes in expression was assessed using a Student's *t*-test or two-way ANOVA, as indicated in the figure legends.

PCR array. A PCR array kit (QIAGEN; catalog no. PAM126Z) was used to assess the expression of 84 genes involved in mechanisms of synaptic plasticity, using cDNA obtained from the hippocampi of AdFNDC5-infected (or AdGFP-infected) mice subsequently infused intracerebroventricularly with AβOs (or vehicle). Hippocampi were dissected 7 days after AβO injection. The assay was conducted according to the manufacturer's instructions, and the results were initially analyzed using volcano plots. Independent validation of differentially expressed genes was carried out by qPCR. Statistical significance of changes in expression was assessed using a two-way ANOVA.

Immunoblotting and in vitro plate-binding assay. Hippocampi or mature hippocampal cultures were homogenized in radioimmunoprecipitation assay (RIPA) buffer containing protease and phosphatase inhibitor cocktails, and were resolved on 4–20% polyacrylamide precast gels (Invitrogen) with Tris/glycine/SDS buffer run at 200 V for 60 min at room temperature. The gel (30 µg total protein per lane) was electroblotted onto Hybond ECL nitrocellulose membrane using 25 mM Tris, 192 mM glycine, 20% (v/v) methanol, pH 8.3, at 350 mA for 90 min at 4 °C. Membranes were blocked with commercial blocking solution (Licor) for 1 h at room temperature. For experiments with blocking peptide, anti-FNDC5 antibody was preincubated with molar ratio excess of recombinant irisin (5:1 or 10:1) for 3 h at room temperature before incubation with membranes. Primary antibodies (anti-FNDC5, anti-BDNF, anti-GAPDH (1:1,000), anti-β-actin monoclonal antibodies (1:20,000)) were diluted in blocking solution and incubated with the membranes overnight at 4 °C. After incubation with secondary anti-mouse or anti-rabbit IgGs (1:10,000 in TBST) for 60 min, membranes were washed, developed with SuperSignal West Femto Maximum Sensitivity substrate (Thermo Fisher Scientific) and imaged on photographic film. For Odyssey fluorescent detection, membranes were incubated with fluorescent IRDye-conjugated antibodies (1:10,000) for 60 min, washed, and scanned in an Odyssey detector. Optical density determination for quantification was performed on ImageJ. The in vitro plate-binding assay was performed as described previously[68].

Protein synthesis (SUnSET). Nonradioactive metabolic labeling by puromycin incorporation was performed to detect newly synthesized peptides, as described previously[30,69]. Briefly, hippocampal cultures were exposed to 1 µM puromycin for 30 min before experimental endpoints and harvested in RIPA buffer. Puromycin incorporation, used as a proxy of protein synthesis rate, was detected using 12D10 anti-puromycin antibody (1:20,000). Densitometric analysis was performed in whole lanes (from 10 to 180 kDa), and β-actin was used as a loading control.

Determination of cAMP levels. cAMP was measured radiometrically, as described previously[70]. Briefly, human cortical slices were exposed to irisin (25 nM; 45 min) in the presence of the phosphodiesterase inhibitor 3-isobutyl-1-methylxanthine (500 µM) added 30 min before irisin.

ELISA. Tissue samples were homogenized in 100 mM Tris, 150 mM NaCl, 1 mM EGTA, 1 mM EDTA, and 1% Triton X-100, supplemented with protease and phosphatase inhibitor cocktails. Blood was obtained by cardiac puncture, collected in heparin-coated low-protein-adsorption plastic tubes, centrifuged, and plasma fractions were either freshly used for ELISA or immediately frozen in liquid nitrogen and stored at −80 °C until analysis. Soluble $A\beta_{42}$ was measured in the supernatant, while insoluble $A\beta_{42}$ was recovered by rehomogenizing the pellet in 6 M guanidine hydrochloride for 1 h. $A\beta_{42}$, BDNF, cAMP, CREB, and irisin ELISA assays were performed according to the manufacturer's instructions, after sample dilution optimization.

Mouse genotyping. Animals were genotyped before the studies using specific primers. APP/PS1 ΔE9 and APP/PS1 M146L genotyping was carried out according to standard protocols. Briefly, genomic DNA was extracted from sections of mice tails and subjected to amplification using specific forward and reverse primers for the respective transgenic construct. Thermal cycling consisted of 35 cycles at 94 °C for 1 min, 52 °C for 1 min, and 72 °C for 1 min. PCR products were resolved on a 1.5% agarose gel, evidencing specific bands for transgenic animals after ethidium bromide staining.

Statistical analysis. All analyses were performed with Prism (GraphPad) and datasets were assessed for normality and group variance before statistical testing. Values are expressed as mean ± s.e.m. unless otherwise stated. Two-tailed statistical tests are indicated in each figure ($^*P<0.05$; $^{**}P<0.01$); post-test corrections were used every time multiple comparisons were performed (as indicated in each figure).

Study design and approval. The sample size for each experiment was estimated by performing pilot studies and by previous experience with different experimental approaches. No algorithm or software was used to randomize animal subjects. Animal subjects were assigned to experimental groups by the researcher. Experiments involving irisin detection in human CSF, dendritic spine quantification in neuronal cultures, LTP experiments, and behavioral experiments in mice were performed in a blind fashion. All procedures involving animal research were in compliance with international standards and were approved by the Institutional Animal Care and Use Committee of the Federal University of Rio de Janeiro (protocols nos. IBqM 022, IBqM 041, IBqM 055). Experiments performed at Columbia University Medical Center were approved by the Institutional Animal Care and Use Committee under protocol no. AC-AAAE9652. Procedures involving human cortical tissue were approved by the National Committee for Research Ethics (CONEP) of the Brazilian Ministry of Health (protocol no. 0069.0.197.000-05). Donors gave written informed consent for use of their brain tissue, which would otherwise have been discarded following surgeries. All experimental procedures involving postmortem human brain tissue were in compliance with the University of Kentucky IRB. Experimental procedures involving human CSF were approved by the Committee for Research Ethics of Copa D'Or Hospital (protocol no. 47163715.0.0000.5249). Donors gave written informed consent for use of brain tissue or CSF. All animal and human studies have been performed according to international ethical regulations and standards. More details can be found in the Life Sciences Reporting Summary.

Reporting Summary. Further information on research design is available in the Nature Research Reporting Summary linked to this article.

Data availability

Mass spectrometry raw data (Fig. 1 and Extended Data Fig. 1) and full blots (Fig. 2 and Extended Data Figs. 3,4, and 10) are available as source data files accompanying this article. Additional data that support the findings of this study are available from the corresponding author upon reasonable request. Requests of datasets obtained from human research will be subject to additional review steps by the IRB that has granted permit for a particular research. Please contact the corresponding authors for additional information.

References

53. Smith, R. W., Wang, J., Bucking, C. P., Mothersill, C. E. & Seymour, C. B. Evidence for a protective response by the gill proteome of rainbow trout exposed to X-ray induced bystander signals. *Proteomics* **7**, 4171–4180 (2007).
54. Mendes, N. D. et al. Free-floating adult human brain-derived slice cultures as a model to study the neuronal impact of Alzheimer's disease-associated Aβ oligomers. *J. Neurosci. Meth.* **307**, 203–209 (2018).
55. Drummond, C. et al. Deficits in narrative discourse elicited by visual stimuli are already present in patients with mild cognitive impairment. *Front. Aging Neurosci.* **7**, 96 (2015).
56. Ledo, J. H. et al. Amyloid-β oligomers link depressive-like behavior and cognitive deficits in mice. *Mol. Psychiatry* **18**, 1053–1054 (2013).
57. Ledo, J. H. et al. Cross talk between brain innate immunity and serotonin signaling underlies depressive-like behavior induced by Alzheimer's amyloid-β oligomers in mice. *J. Neurosci.* **36**, 12106–12116 (2016).
58. Trinchese, F. et al. Inhibition of calpains improves memory and synaptic transmission in a mouse model of Alzheimer disease. *J. Clin. Invest.* **118**, 2796–2807 (2008).
59. Alamed, J., Wilcock, D. M., Diamond, D. M., Gordon, M. N. & Morgan, D. Two-day radial-arm water maze learning and memory task; robust resolution of amyloid-related memory deficits in transgenic mice. *Nat. Protoc.* **1**, 1671–1679 (2006).
60. Puzzo, D. et al. Phosphodiesterase 5 inhibition improves synaptic function, memory, and amyloid-β load in an Alzheimer's disease mouse model. *J. Neurosci.* **29**, 8075–8086 (2009).
61. Madeira, C. et al. d-serine levels in Alzheimer's disease: implications for novel biomarker development. *Transl. Psychiatry* **5**, e561 (2015).
62. Seixas Da Silva, G. S. et al. Amyloid-β oligomers transiently inhibits AMP-activated kinase and cause metabolic defects in hippocampal neurons. *J. Biol. Chem.* **292**, 7395–7406 (2017).
63. Gong, B. et al. Ubiquitin hydrolase Uch-L1 rescues β-amyloid-induced decreases in synaptic function and contextual memory. *Cell* **126**, 775–788 (2006).
64. De Felice, F. G. et al. Aβ oligomers induce neuronal oxidative stress through an *N*-methyl-D-aspartate receptor-dependent mechanism that is blocked by the Alzheimer drug memantine. *J. Biol. Chem.* **282**, 11590–11601 (2007).
65. Lambert, M. P. et al. Monoclonal antibodies that target pathological assemblies of Aβ. *J. Neurochem.* **100**, 23–35 (2007).
66. Abràmoff, M. D., Magalhães, P. J. & Ram, S. J. Image processing with ImageJ. *Biophotonics Int.* **11**, 36–42 (2004).
67. Livak, K. J. & Schmittgen, T. D. Analysis of relative gene expression data using real-time quantitative PCR and the $2^{-\Delta\Delta C_T}$ method. *Methods* **25**, 402–408 (2001).
68. Brito-Moreira, J. et al. Interaction of amyloid-β (Aβ) oligomers with neurexin 2α and neuroligin 1 mediates synapse damage and memory loss in mice. *J. Biol. Chem.* **292**, 7327–7337 (2017).
69. Schmidt, E. K., Clavarino, G., Ceppi, M. & Pierre, P. SUnSET, a nonradioactive method to monitor protein synthesis. *Nat. Methods* **6**, 275–277 (2009).
70. Beckman, D. et al. Prion protein modulates monoaminergic systems and depressive-like behavior in mice. *J. Biol. Chem.* **290**, 20488–20498 (2015).

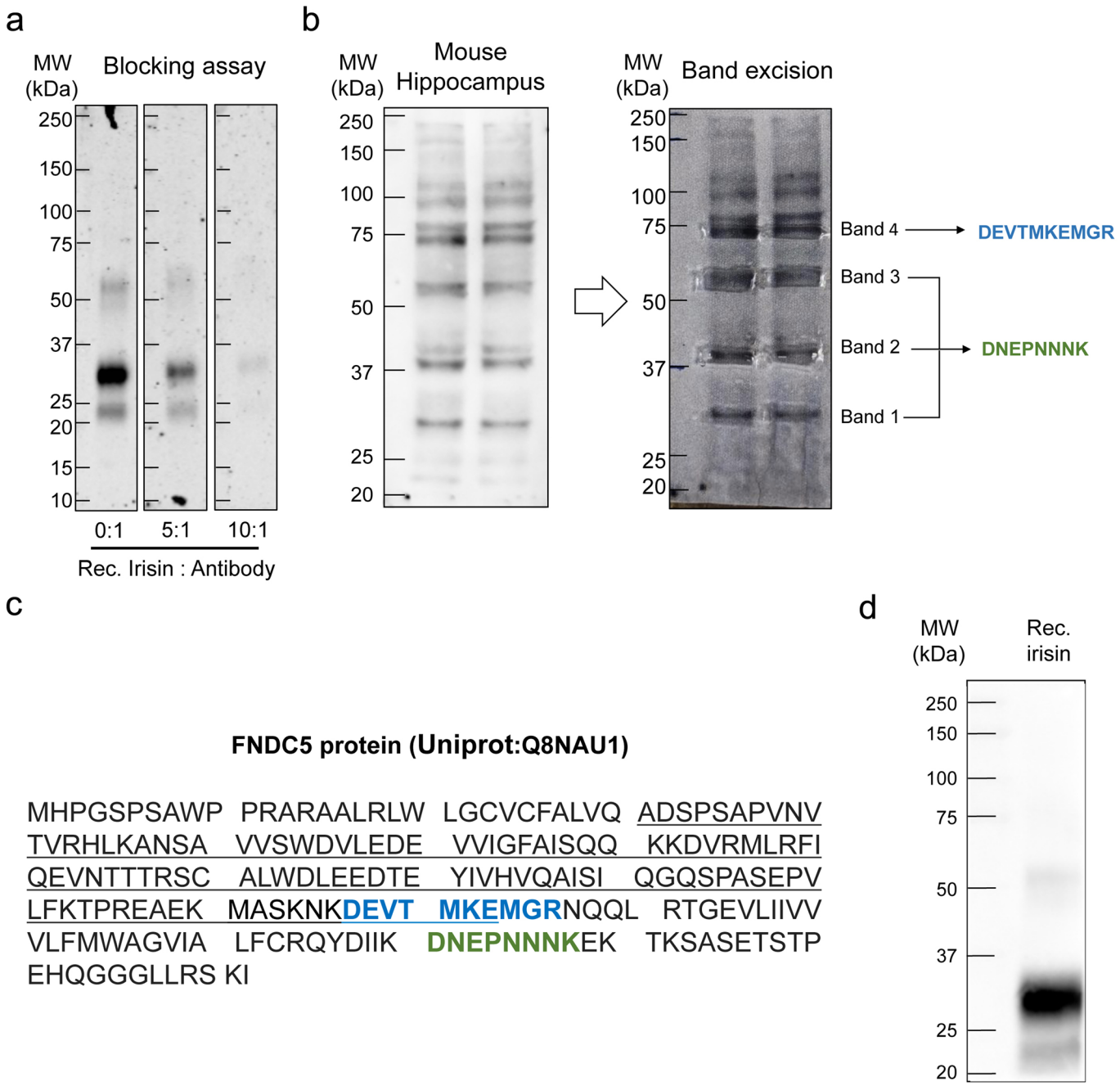

Extended Data Fig. 1 | Validation of anti-FNDC5 for detection of brain FNDC5/irisin. **a**, Antibody blocking assay. Previous incubation of anti-FNDC5 (Abcam; ab131390) with increasing molar ratios of recombinant irisin (Adipogen; AG-40B-0136) reduces the signal of recombinant irisin detected by immunoblotting. The experiment was repeated 4 times with similar results. **b**, Left, Immunoblot of mouse hippocampus homogenate probed with anti-FNDC5. Immunolabeled bands 1–4 (see Results) were used to guide excision of the corresponding bands from the other half of the SDS-PAGE gel that had not been electroblotted (right). Band excision was guided by overlaying the unstained gel onto an image of the developed immunoblot (right panel). Excised bands were subjected to in-gel tryptic digestion followed by mass spectrometry analysis, as described in the Methods. Peptides identified by mass spectrometry in each band are indicated. **c**, Full-length FNDC5 amino acid sequence. The sequence corresponding to irisin is underlined. Peptides identified by mass spectrometry in excised bands are highlighted in green (bands 1, 2 and 3) or blue (band 4). **d**, Antibody used in the Phoenix ELISA kit (EK-067-29) recognizes recombinant irisin expressed in CHO cells (Adipogen; AG-40B-0136). The experiment was repeated 3 times with similar results. See Source Data 1 for original data.

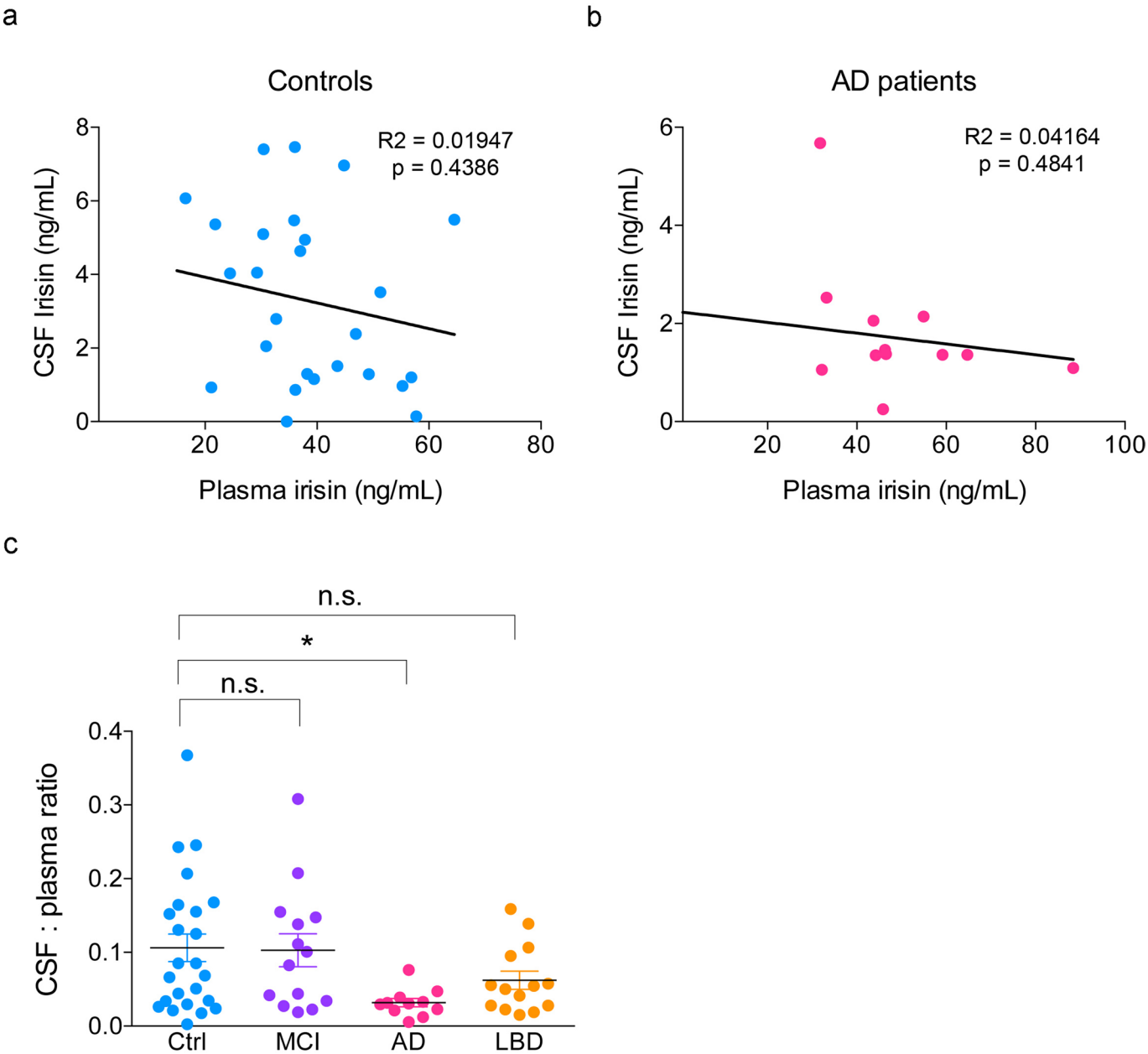

Extended Data Fig. 2 | CSF and plasma irisin correlations. a,**b**, CSF:plasma irisin levels correlation in controls ($N=26$) (**a**) or AD patients (**b**) ($N=14$; lines represent linear regression fits to the data; r^2 and P values as indicated in the figure). **c**, CSF to plasma irisin ratio is selectively reduced in AD patients, as compared to controls, MCI or LBD patients ($N=26$ controls, 14 MCI, 11 AD, 13 LBD cases). Data are shown as mean ± s.e.m., $^*P<0.05$; One-way ANOVA with Holm-Sidak post-test.

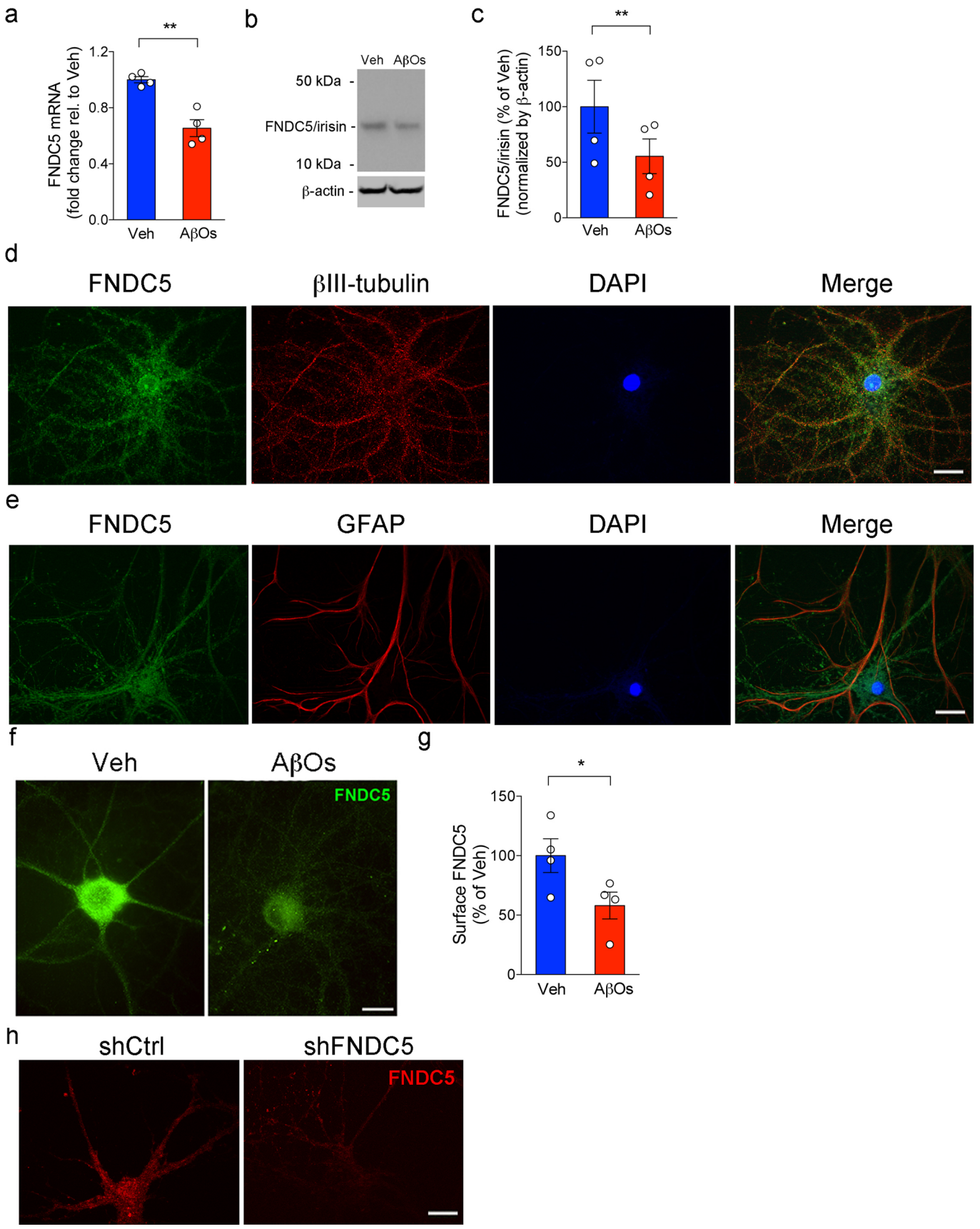

Extended Data Fig. 3 | See next page for caption.

Extended Data Fig. 3 | AβOs reduce FNDC5/irisin levels in hippocampal neurons. a–**c**, Primary cultured hippocampal neurons were exposed to 500 nM AβOs for 24 h. Fndc5 mRNA (**a**) and FNDC5/irisin protein levels (**b**,**c**) in cultured hippocampal neurons exposed or not to AβOs ($N = 4$ experiments with independent neuronal cultures and AβO preparations; data are shown as mean ± s.e.m., $^{**}P < 0.01$; paired Student's *t*-test; two-sided). See Source Data 5 for original data. **d**,**e**, Colocalization of surface FNDC5 immunoreactivity (green) with β-tubulin III (red) immunoreactivity in cultured hippocampal neurons (**d**). Colocalization of surface FNDC5 immunoreactivity (green) with glial fibrillary acidic protein (GFAP) (red) (**e**). The experiment was repeated 2 times with similar results in independent cultures. **f**,**g**, Primary cultured hippocampal neurons were exposed to 500 nM AβOs for 24 h. **g**, Summary quantification of surface FNDC5 immunoreactivity in cultured neurons ($N = 4$ experiments with independent neuronal cultures and AβO preparations; 30 images (from 2–3 coverlips) per condition per experiment. Data are shown as mean ± s.e.m. $^{*}P < 0.05$, paired Student's t-test; two-sided). **h**, Surface FNDC5 immunoreactivity (red) in 18 DIV cultured hippocampal neurons after lentiviral knockdown of FNDC5 (shFNDC5) ($N = 2$ experiments with independent cultures; 30 images (from 2–3 coverslips) per condition per experiment). Scale bar = 10 mm.

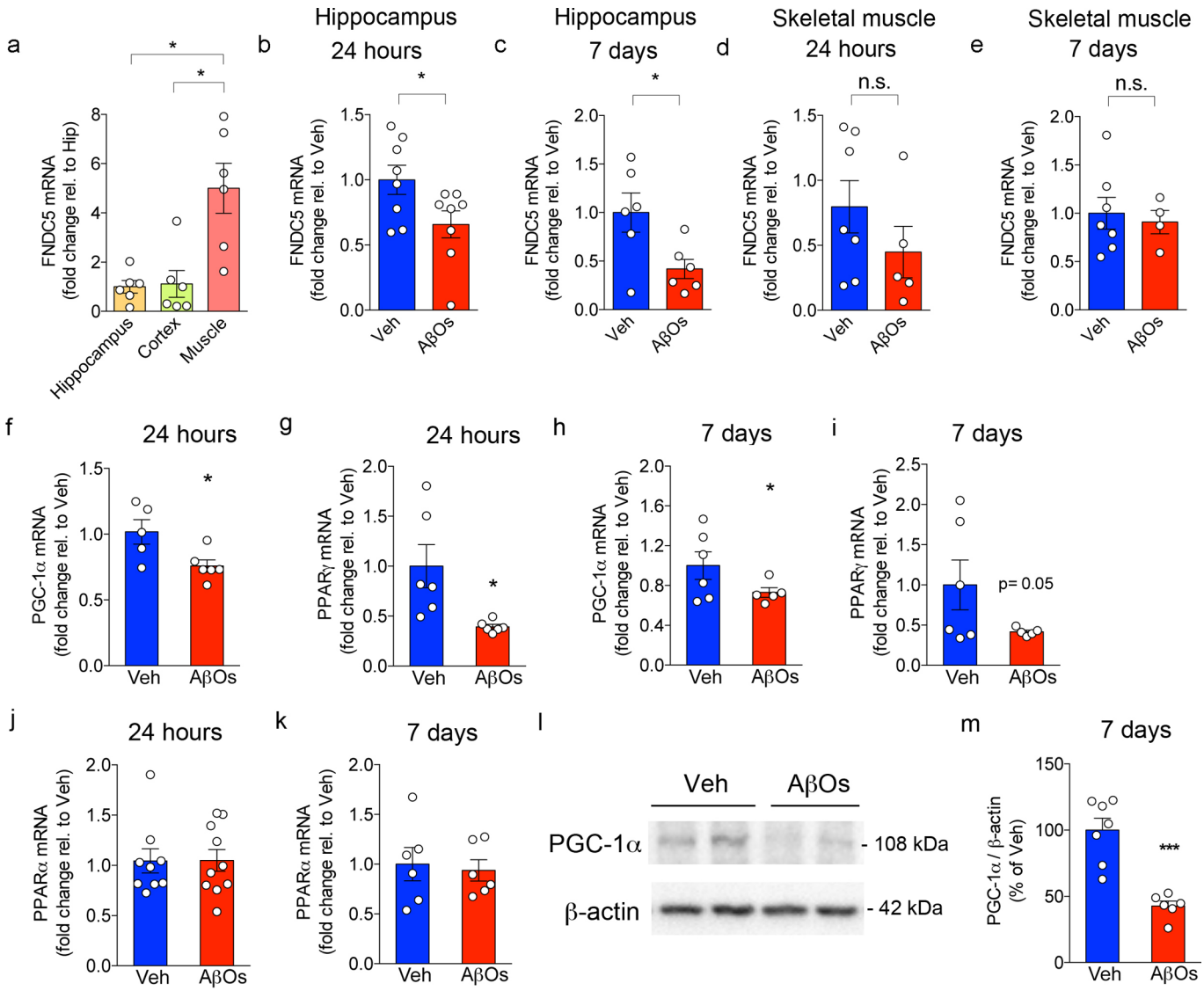

Extended Data Fig. 4 | AβOs reduce hippocampal FNDC5, PGC-1α, and PPARγ expression. a, Hippocampal, cortical, and skeletal muscle (gastrocnemius) expression of FNDC5 in C57BL/6 mice ($N=6$ per group). Data are shown as mean ± s.e.m.; *$P<0.05$; paired one-way ANOVA with Holm-Sidak correction; two-sided. **b**,**c**, Hippocampal FNDC5 mRNA in C57BL/6 i.c.v-infused with 10 pmol AβOs for 24 h ($N=8$ per group) (**b**) or 7 days ($N=5$ per group) (**c**). Data are shown as mean ± s.e.m.; *$P<0.05$; Student's *t*-test; two-sided). **d**,**e**, Skeletal muscle (gastrocnemius) FNDC5 mRNA in C57BL/6 i.c.v-infused with 10 pmol AβOs for 24 h ($N=7$ Veh, 5 AβOs) (**d**) or 7 days ($N=7$ Veh, 4 AβOs) (**e**). Data are shown as mean ± s.e.m.; *$P<0.05$; Student's *t*-test; two-sided). **f**–**k**, Hippocampal mRNA levels of PGC-1α (**f**,**h**), PPARγ (**g**,**i**) and PPARα (**j**,**k**) were measured 24 h or 7 days after infusion, as indicated ($N=5$ per group). mRNA levels were normalized by β-actin expression. (**l**,**m**) AβOs reduced hippocampal PGC-1α protein levels in C57BL/6 mice 7 days after infusion ($N=7$ Veh, 6 AβOs). Data are shown as mean ± s.e.m.; *$P<0.05$; Student's t-test; two-sided). See Source Data 6 for original data.

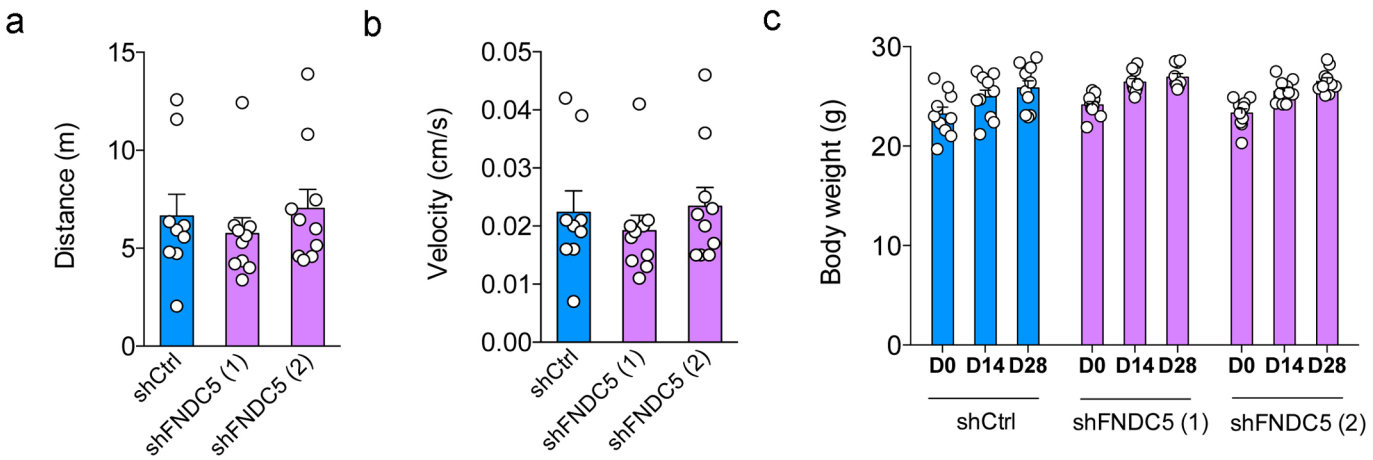

Extended Data Fig. 5 | Lentiviral vectors expressing shFNDC5 did not cause motor impairment or affect body weight gain in mice. a,**b**, Distance traveled (**a**) and mean velocity (**b**) of mice allowed to explore an open field arena for 5 min ($N = 9$ mice for shCtrl, 10 mice each for shFNDC5 (1) and (2) groups). Data are shown as mean ± s.e.m. **c**, Body weight measured 0, 14 or 28 days after lentiviral injections ($N = 10$ mice per group; one-way ANOVA followed by Holm-Sidak post-test). Data are shown as mean ± s.e.m. No significantly statistical difference was found among groups.

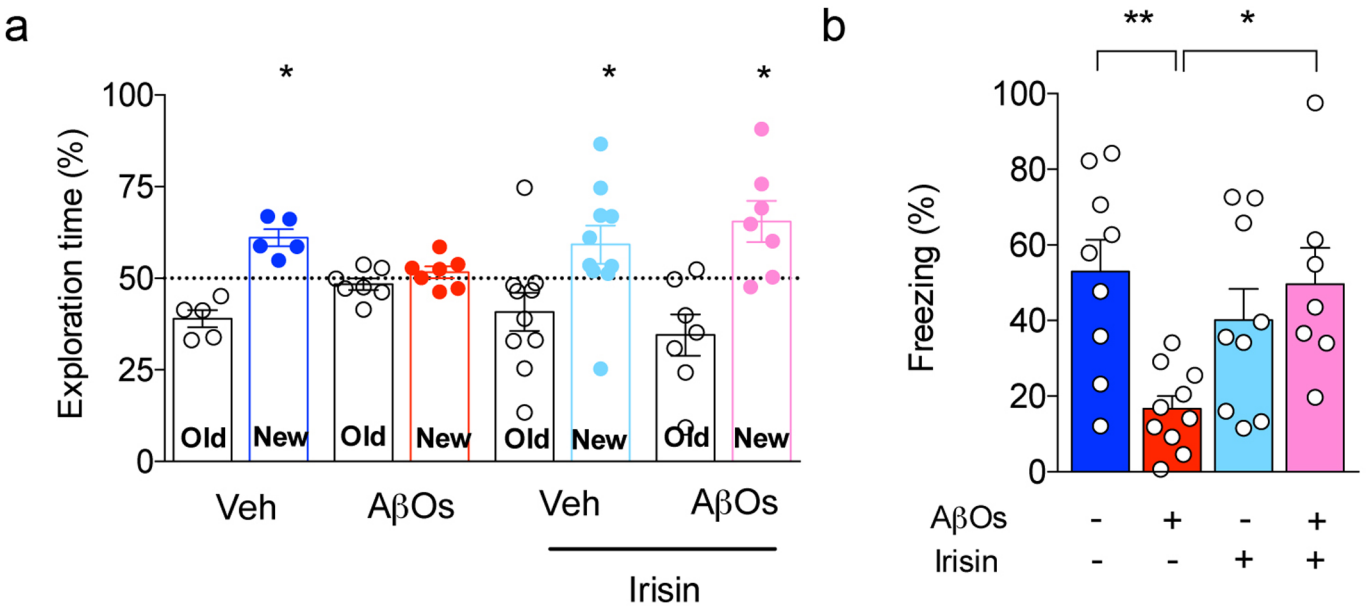

Extended Data Fig. 6 | Intrahippocampal administration of recombinant irisin prevents AβO-induced memory impairment. a,**b**, Male Swiss mice (3 months old) were bilaterally injected with recombinant irisin (75 pmol per hippocampus) and received 10 pmol AβOs i.c.v. Novel object recognition (**a**) and contextual fear conditioning (**b**) tasks (tested 5 days post-infusion of AβOs) ($N = 9$ mice for Veh, 10 for AβOs, 9 for irisin and 7 for AβOs + irisin). Data are shown as mean ± s.e.m. $^*P < 0.05$, two-way ANOVA with Holm-Sidak post-test; two-sided.

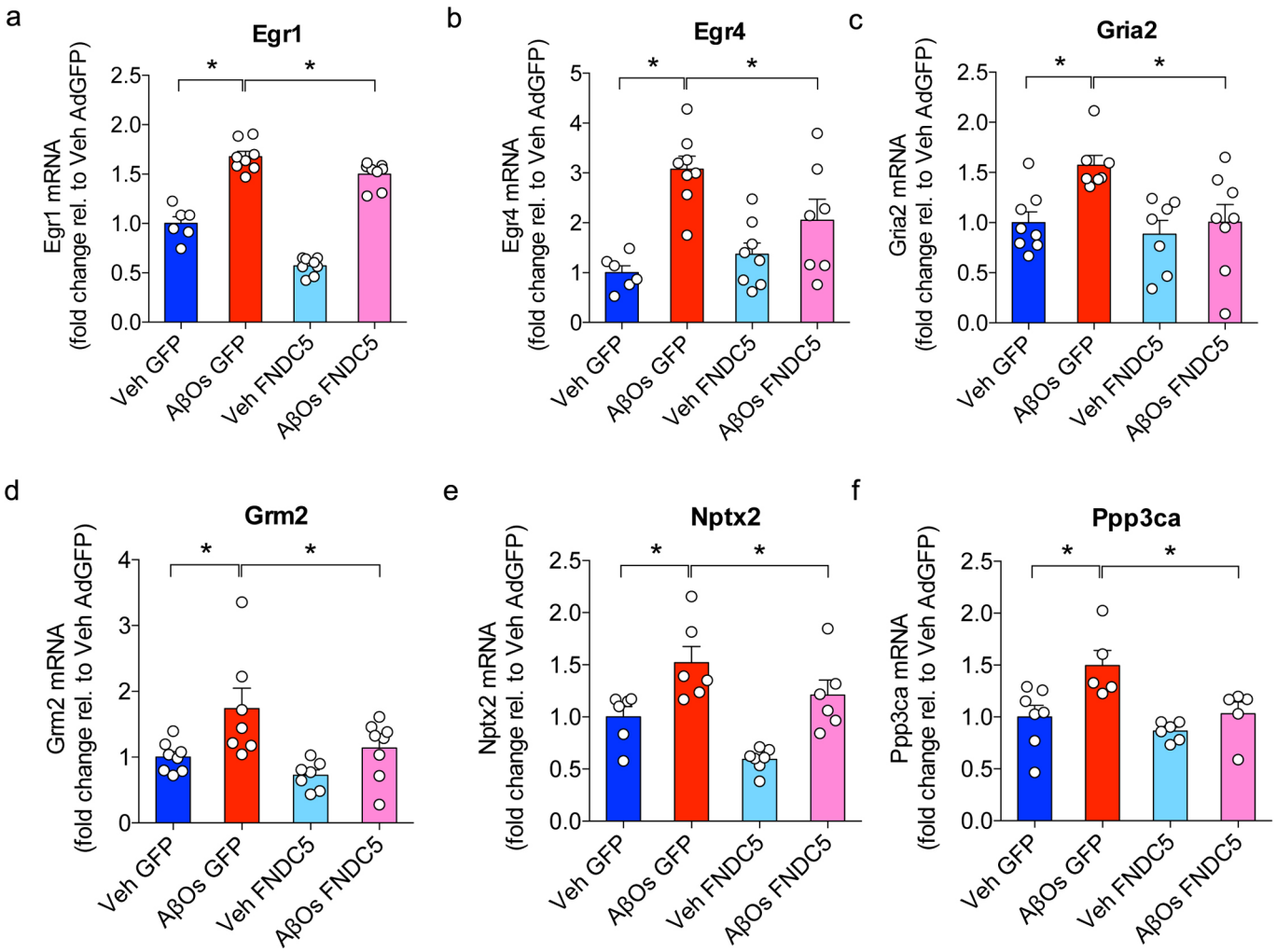

Extended Data Fig. 7 | Validation of PCR array results by qPCR. a–f, AdFNDC5 expression of 6 synapse plasticity-related genes after AβO injection: Egr1 (**a**), Egr4 (**b**), Gria2 (**c**), Grm2 (**d**), Nptx2 (**e**), and Ppp3ca (**f**). $N = 6$ mice per experimental group. Data are shown as mean ± s.e.m. $^*P < 0.05$; two-way ANOVA with Holm-Sidak post-test; two-sided.

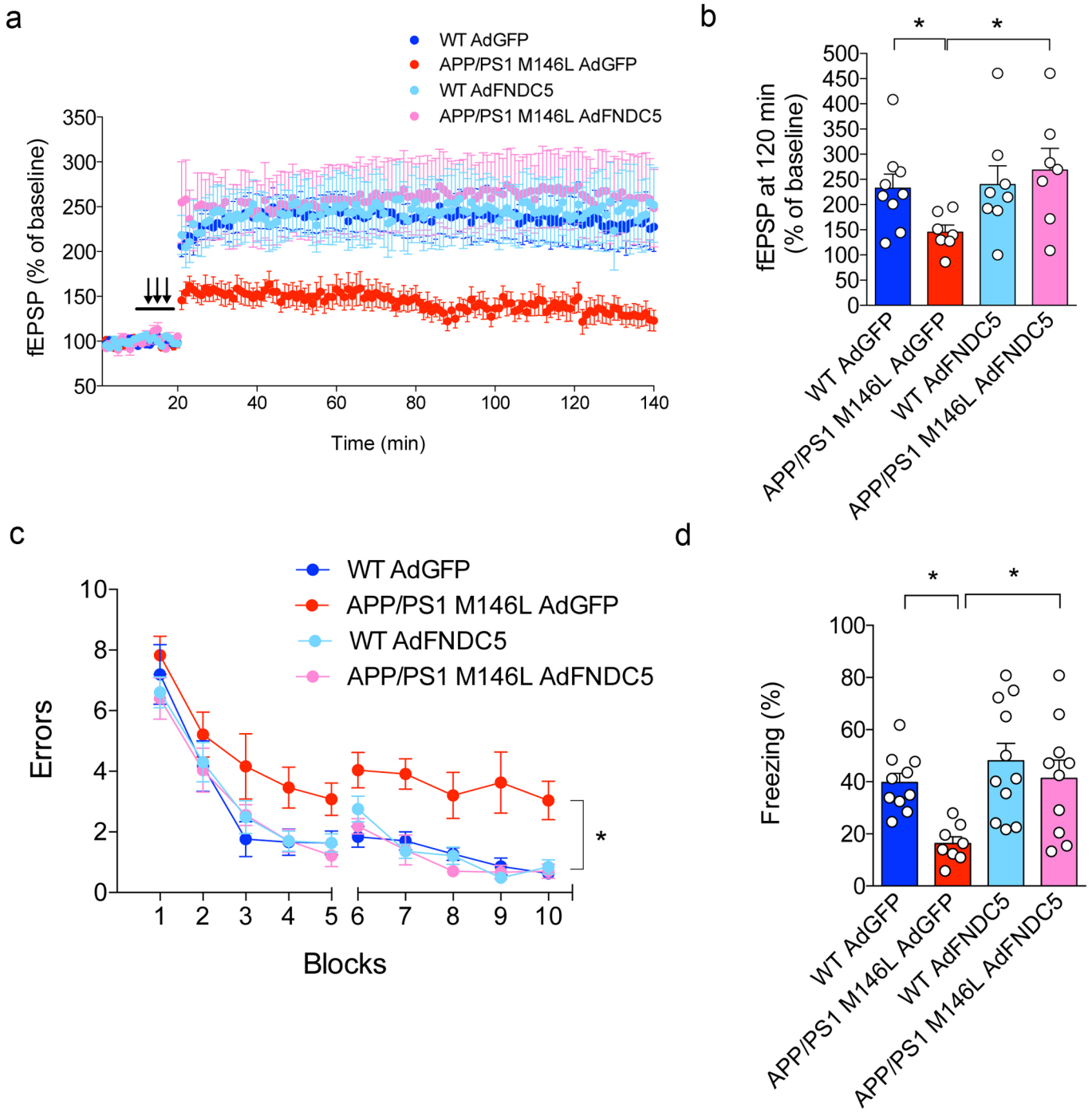

Extended Data Fig. 8 | FNDC5/irisin rescues defective synaptic plasticity and memory in APP/PS1 M146L mice. a–d, APP/PS1 M146L mice (or WT littermates) were injected i.c.v. with an adenoviral vector expressing full-length FNDC5 (AdFNDC5) or green fluorescent protein (AdGFP, used as a control). Hippocampal slices were obtained and subjected to high-frequency stimulation for LTP recordings. Field excitatory postsynaptic potentials (fEPSP) in hippocampal slices from each experimental group (N = 9 slices for vehicle AdGFP, 7 for APP/PS1 M146L AdGFP, 8 for WT AdFNDC5, 7 for APP/PS1 M146L AdFNDC5; from 3–4 animals per group) (**a**). fEPSP at 120 min (**b**). I.c.v.-injected AdFNDC5 rescued memory impairment in 3–4 months-old APP/PS1 M146L mice in 2-day radial arm water maze (**c**) and in contextual fear conditioning (**d**) ($N = 10$ mice for WT GFP, 8 for APP/PS1 GFP, 11 for WT FNDC5, 10 for APP/PS1 FNDC5). Data are shown as mean ± s.e.m. *$P < 0.05$; two-way ANOVA with Holm-Sidak post-test; two-sided.

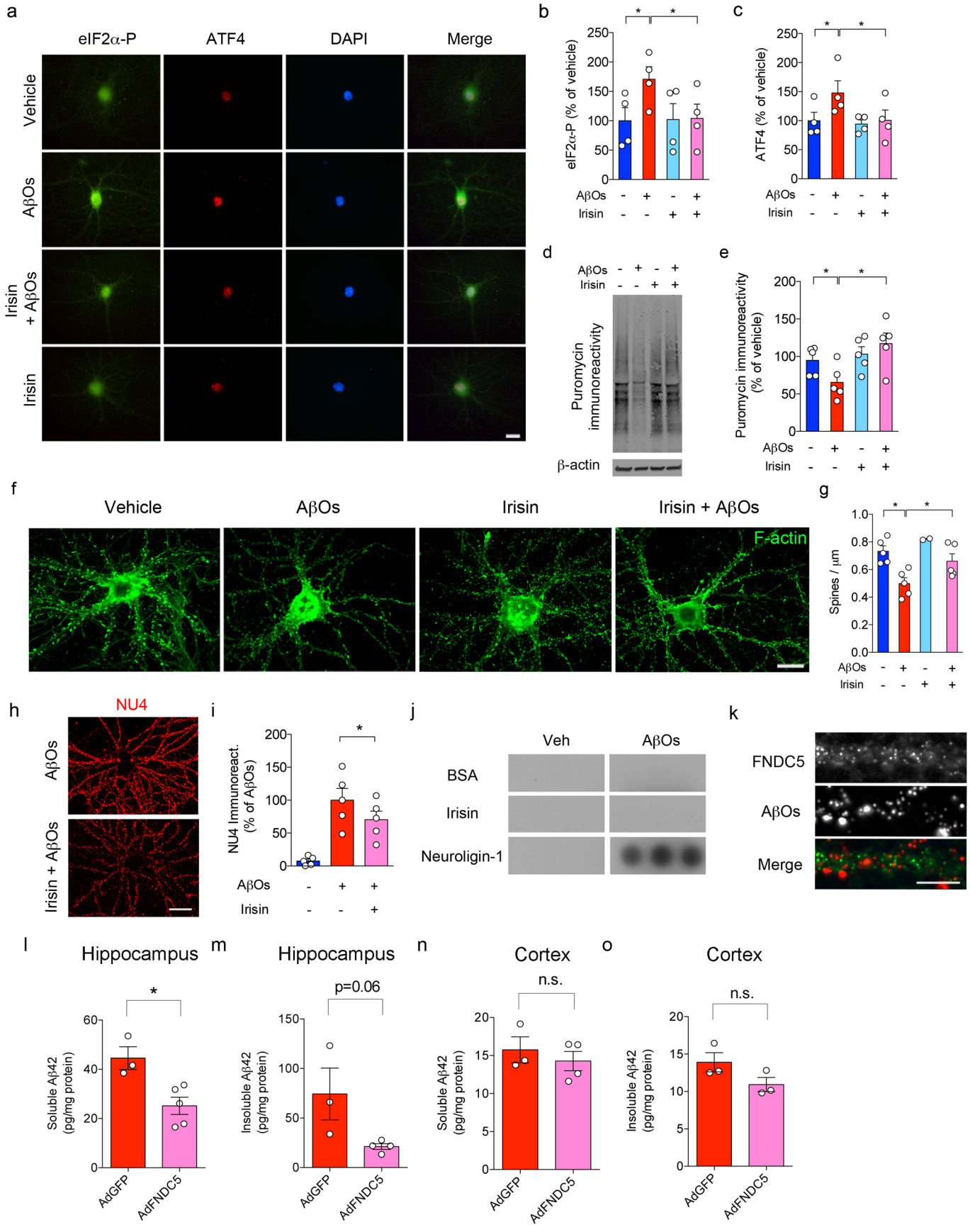

Extended Data Fig. 9 | See next page for caption.

Extended Data Fig. 9 | Irisin counteracts AD-linked activation of cellular stress response and dendritic spine loss in hippocampal neurons. a, Effect of irisin on AβO-induced increases in eIF2α-P (green) and upregulation of nuclear ATF4 (red). Nuclei were counterstained in blue (DAPI). Scale bar = 5 mm. **b**,**c**, Summary quantification of immunocytochemistry experiments ($N = 4$ experiments with independent neuronal cultures and AβO preparations). $^*P < 0.05$; two-way ANOVA with Holm-Sidak correction; two-sided. Data are represented by mean ± s.e.m. **d**,**e**, Summary quantification of of protein synthesis in hippocampal neurons, as measured by non-radioactive puromycin incorporation (SUnSET) normalized by β-actin levels ($N = 4$ experiments with independent hippocampal cultures and AβO preparations). $^*P < 0.05$; two-way ANOVA with Holm-Sidak correction; two-sided. Data are represented by mean ± s.e.m. **f**,**g**, Representative images of dendritic spines in hippocampal neurons, as measured by F-actin labeling with Alexa-conjugated phalloidin ($N = 5$ experiments with independent neuronal cultures and AβO preparations). Scale bar = 20 mm. $^*P < 0.05$, two-way ANOVA. Data are shown as mean ± s.e.m. At least 30 neurons were analyzed per condition per experiment in immunocytochemistry experiments. **h**, AβO binding to cultured hippocampal neurons, as detected by AβO-sensitive antibody NU4 (red), after treatment with recombinant irisin (25 nM). Scale bar, = 10 mm. The experiments were repeated 5 times with similar results. **i**, Summary quantification of 5 experiments with independent neuronal cultures and AβO preparations. Data are shown as mean ± s.e.m. $^*P < 0.05$; paired one-way ANOVA; two-sided. **j**, AβO interaction with different proteins in a plate-binding assay. BSA was used as a negative control, while neuroligin-1 was used as a positive control ($N = 3$ experiments with independent AβO preparations)[68]. Representative dots were cropped from the same film. See Source Data 7 for original data. **k**, Double immunocytochemistry colocalization between AβOs (red) and surface FNDC5 (green) in primary cultured hippocampal neurons (3 experiments with independent neuronal cultures and AβO preparations, with 20–25 images (from 2–3 coverslips) per experiment). Scale bar = 5 mm. The experiments were repeated 3 times with similar results. **l**–**o**, Levels of soluble (**l**,**n**) and insoluble $A\beta_{42}$ (**m**,**o**) in hippocampus ($N = 3$ for AdGFP, 5 for AdFNDC5) and cortex ($N = 3$ for AdGFP, 4 for AdFNDC5) of APP/PS1 M146L mice. Data are shown as mean ± s.e.m. $^*P < 0.05$; Student's *t*-test; two-sided.

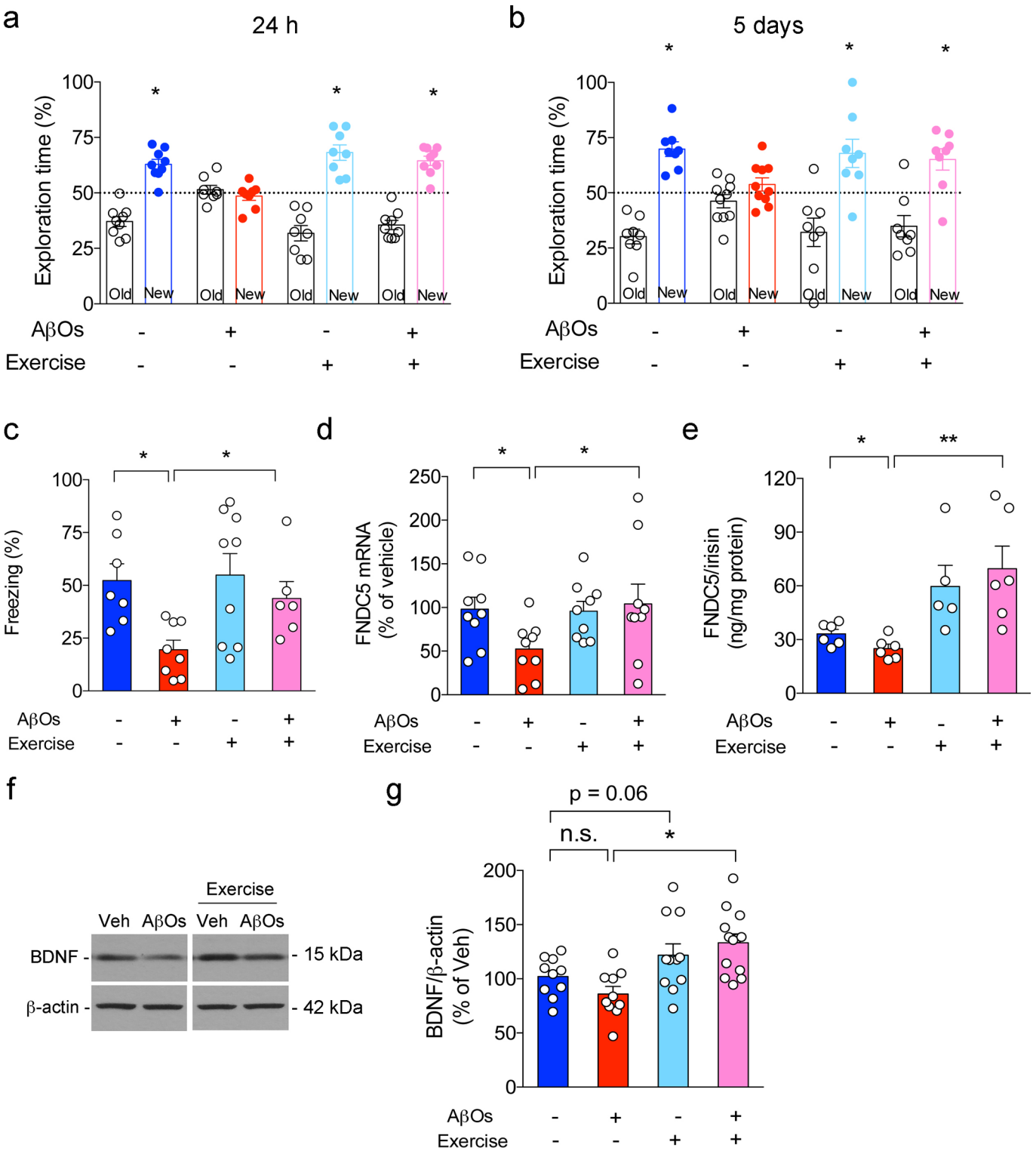

Extended Data Fig. 10 | Exercise blocks AβO-induced memory impairment in mice. Effect of exercise (swimming; 5 weeks, 5 days/week, 1 h/day) on memory impairment induced by i.c.v. infusion of AβOs in Swiss mice. **a**–**c**, Novel object recognition assessed 24 h ($N = 9$ mice for vehicle, 8 for AβOs, 8 for exercise, 9 for exercise + AβOs) (**a**) or 5 days post-infusion of AβOs ($N = 8$ mice for vehicle, 10 for AβOs, 8 for exercise and 8 for exercise + AβOs) (**b**). Data are shown as mean ± s.e.m. $^{*}P < 0.05$; one-sample Student's *t*-test. Contextual fear conditioning (**c**) assessed 7 days post-infusion of AβOs ($N = 7$ mice for vehicle, 8 for AβOs, 9 for exercised and 6 for exercised + AβOs). $^{*}P > 0.05$; two-way ANOVA followed by Holm-Sidak post-test; two-sided). **d**,**e**, Hippocampal FNDC5 mRNA (**d**) ($N = 9$ mice per group) and FNDC5/irisin protein levels (**e**; measured by ELISA) after 5 weeks of exercise ($N = 6$ mice each for vehicle, AβOs and exercise + AβOs, and 5 for exercise) in male Swiss mice that received 10 pmol AβOs i.c.v. **f**,**g**, Hippocampal BDNF levels in exercised mice ($N = 10$ mice for vehicle and AβOs, 11 for exercise, 13 for exercise + AβOs). Data are shown as mean ± s.e.m. $^{*}P < 0.05$; $^{**}P < 0.01$, two-way ANOVA followed by Holm-Sidak post-test; two-sided. Representative bands were cropped from the same membrane. See Source Data 8 for original data.

nature research

Corresponding author(s): Fernanda De Felice, Sergio Ferreira and Ottavio Arancio

Reporting Summary

Nature Research wishes to improve the reproducibility of the work that we publish. This form provides structure for consistency and transparency in reporting. For further information on Nature Research policies, see Authors & Referees and the Editorial Policy Checklist.

Statistical parameters

When statistical analyses are reported, confirm that the following items are present in the relevant location (e.g. figure legend, table legend, main text, or Methods section).

n/a	Confirmed	
☐	☒	The exact sample size (*n*) for each experimental group/condition, given as a discrete number and unit of measurement
☐	☒	An indication of whether measurements were taken from distinct samples or whether the same sample was measured repeatedly
☐	☒	The statistical test(s) used AND whether they are one- or two-sided *Only common tests should be described solely by name; describe more complex techniques in the Methods section.*
☐	☒	A description of all covariates tested
☐	☒	A description of any assumptions or corrections, such as tests of normality and adjustment for multiple comparisons
☐	☒	A full description of the statistics including central tendency (e.g. means) or other basic estimates (e.g. regression coefficient) AND variation (e.g. standard deviation) or associated estimates of uncertainty (e.g. confidence intervals)
☐	☒	For null hypothesis testing, the test statistic (e.g. *F*, *t*, *r*) with confidence intervals, effect sizes, degrees of freedom and *P* value noted *Give P values as exact values whenever suitable.*
☒	☐	For Bayesian analysis, information on the choice of priors and Markov chain Monte Carlo settings
☒	☐	For hierarchical and complex designs, identification of the appropriate level for tests and full reporting of outcomes
☒	☐	Estimates of effect sizes (e.g. Cohen's *d*, Pearson's *r*), indicating how they were calculated
☐	☒	Clearly defined error bars *State explicitly what error bars represent (e.g. SD, SE, CI)*

Our web collection on statistics for biologists may be useful.

Software and code

Policy information about availability of computer code

Data collection	ANY-Maze 2, Noldus Ethovision XT, Zeiss Axiovision 4.8, pClamp 10 (Molecular Devices), Microsoft Office 2008 for Mac, Li-cor Image Studio 3.0, SpectaMax Softmax Pro 6, Applied Biosystems 7500 Real-Time PCR software.
Data analysis	ANY-Maze 2, Noldus Ethovision XT, Zeiss Axiovision 4.8, pClamp 10 (Molecular Devices), Microsoft Office 2008 for Mac, GraphPad Prism 6, Fiji 3.0, Applied Biosystems 7500 Real-Time PCR software, Qiagen RT2 Data Profiler.

For manuscripts utilizing custom algorithms or software that are central to the research but not yet described in published literature, software must be made available to editors/reviewers upon request. We strongly encourage code deposition in a community repository (e.g. GitHub). See the Nature Research guidelines for submitting code & software for further information.

Data

Policy information about availability of data

All manuscripts must include a data availability statement. This statement should provide the following information, where applicable:

- Accession codes, unique identifiers, or web links for publicly available datasets
- A list of figures that have associated raw data
- A description of any restrictions on data availability

Mass spectrometry raw data (Figure 1; Extended Data Figure 1) and full blots (Figure 2; Extended Data Figures 3,4 and 10) are available as source data files

accompanying this paper. Additional data that support the findings of this study are available from the corresponding author upon reasonable request. Requests of datasets obtained from human research will be subject to additional reviews steps by the Institutional Review Board who has granted permit for a particular research. Please contact the corresponding authors for additional information.

Field-specific reporting

Please select the best fit for your research. If you are not sure, read the appropriate sections before making your selection.

☒ Life sciences ☐ Behavioural & social sciences ☐ Ecological, evolutionary & environmental sciences

For a reference copy of the document with all sections, see nature.com/authors/policies/ReportingSummary-flat.pdf

Life sciences study design

All studies must disclose on these points even when the disclosure is negative.

Sample size	Sample size for each experiment was estimated by performing pilot studies and by previous experience with different experiments. The rationale was to obtain robust measurements according to the type of experiment, taking variability into consideration. For some experiments, power analyses were performed prior to the start.
Data exclusions	In NOR tests, animals were excluded from the analyses if they had less than 8s of total exploration in the training or the testing phase. This was pre-established. No other exclusion criteria was employed in animal studies.
Replication	Studies involved replication of experimental findings whenever possible. Behavioral tests were performed in different cohorts of animals. Culture experiments were performed independent cultures. We did not have failed replications in the experiments presented in this study.
Randomization	No algorithm or software was used to randomize animal subjects. Animals were randomly assigned to groups by trained researchers performing each experiment.
Blinding	Experiments involving image analyses, electrophysiology, and behavioral tests in mice were performed in blinded fashion.

Reporting for specific materials, systems and methods

Materials & experimental systems

n/a	Involved in the study
☒	☐ Unique biological materials
☐	☒ Antibodies
☒	☐ Eukaryotic cell lines
☒	☐ Palaeontology
☐	☒ Animals and other organisms
☐	☒ Human research participants

Methods

n/a	Involved in the study
☒	☐ ChIP-seq
☒	☐ Flow cytometry
☒	☐ MRI-based neuroimaging

Antibodies

Antibodies used	anti-ATF4 antibody (Sigma, #WH0000468M1, monoclonal, clone 2B3, 1:500), anti-eIF2α–P (phosphoS51) (Enzo Life Sciences, #BML-SA405-100, polyclonal 1:500), anti-eIF2α (total) (Enzo Life Sciences, #ADI-KAP-CP130, polyclonal, 1:400), anti-puromycin (12D10) (EMD Millipore, #MABE343, monoclonal, clone 12D10, 1:5000), anti-FNDC5 (Abcam, #ab131390, polyclonal, 1:500), anti-β-actin (Abcam, #ab8226, monoclonal, clone 8226, 1:20000), anti-GAPDH (Abcam, #ab9485, polyclonal, 1:2000), Tuj1 (R&D, #MAB1195, monoclonal, clone Tuj1), anti-BDNF (Santa Cruz, #sc546, polyclonal, 1:500).
Validation	Antibodies were used according to manufacturer's instructions. Antibody validation for the species/application can be found at the suppliers' webpage. Additional validation for the anti-FNDC5 antibody by immunoblotting and mass spectrometry is present in Extended Data Figure 1 and in Source Data.

Animals and other organisms

Policy information about studies involving animals; ARRIVE guidelines recommended for reporting animal research

Laboratory animals	This work involved use of 3-month old male WT C57BL/6 or Swiss mice, as reported in each figure. In experiments involving transgenic APP/PS1 mice (on a C57BL/6 background) , both males and females were used, and were aged 6-13 month-old.

Wild animals	This study did not involve wild animals.
Field-collected samples	This study did not involve samples collected from field research.

Human research participants

Policy information about studies involving human research participants

Population characteristics	Healthy cortical tissue was obtained from patients with drug-resistant temporal lobe epilepsy subjected to surgical interventions for removal of epileptic foci. Donors were two males (aged 37 and 49 year-old) and three female (aged 18, 39 and 66 year-old). AD tissue was from symptomatic individuals with clinical and pathological features described in Supplementary Table 1. All subjects were categorized by MMSE as control (26-30), early AD (20-25), and late AD (13-17). Sample groups were separated so as to clearly define differences in content of proteins of interest and MMSE score. Cerebrospinal fluid (CSF) or plasma from control and AD patients was collected after extensive neuropsychological investigation supervised by a board-certified psychiatrist, as described. The study cohort included males and females. Age (mean ± SD), in years, was distributed as follows: Controls (67.5 ± 4.9), MCI (71.5 ± 5.8), AD (72.5 ± 8.1), and LBD (71.6 ± 7.0).
Recruitment	For the CSF study, patients were recruted by the IDOR memory clinic after subjective memory complaints, as reported in Methods. For the ex vivo human cortical slices, patients were subjected to lobectomy after extensive clinical examination and explicit diagnosis of refractory epilepsy by board-certified neurologists at the University Hospital. Brain tissue would be otherwise discarded. All studies are in compliance with local and international regulations, and were approved by competent ethics committees. In all cases, diagnosis was defined by board-certified neurology committees, and there is no anticipated potential bias during selection.